Lappeenranta University of Technology

LUT Chemistry

Bachelor's Thesis

Otto Rossi

Simulation of adsorption column for removal of heavy metals from water

18.4.2013

LIST OF SYMBOLS

A	Redlich-Peterson model constant, $m^3\ kg^{-1}$
a	particle surface per unit volume of bed, $m^2\ m^{-3}$
a_{BA}	angular coefficient in BDST model, -
B	Redlich-Peterson model constants, $m^3\ kg^{-1}$
b_{BA}	intersection point in BDST, m^{-3}
C_{BET}	BET adsorption isotherm constant, $m^{-3}\ kg^{-1}$
C_{id}	parameter in intraparticle diffusion model, -
c	concentration in fluid, $kg\ m^{-3}$
c_0	concentration of initial metal ion solution $kg\ m^{-3}$
c_b	effluent concentration in breakthrough point, $kg\ m^{-3}$
c_e	equilibrium constant of solute, $kg\ m^{-3}$
c_i	interface concentration, $kg\ m^{-3}$
c_{ML}	adsorbate monolayer saturation concentration, $kg\ m^{-3}$
c_s	adsorbate concentarion in solids, $kg\ m^{-3}$
D_{eff}	effective diffusivity, $m^2\ s^{-1}$
D_m	diffusivity in the fluid, $m^2\ s^{-1}$
D_s	diffusivity in the solid, $m^2\ s^{-1}$
d_p	particle size, m
g	dimensionless Redlich-Peterson parameter, -
K_a	Langmuir constant, $m^3\ kg^{-1}$
K_{BA}	rate constant in BDST model, $kg^{-1}\ s\text{-}^{1}$
K_d	distribution coefficient of the adsorbate, -
K_f	Freundlich constant, $kg^{1-1/n}\ kg^{-1}$
k_1	pseudo-first order diffusion rate constant, $1\ s^{-1}$
k_2	pseudo-second order rate constant, $kg\ kg^{-1}\ s^{-1}$
k_f	the external mass transfer coefficient between the fluid and the particles in packed bed, $m\ s^{-1}$
k_{id}	intra-particle diffusion rate constant, $kg\ kg^{-1}\ s^{-0,5}$

L	length of column, m
L_{UB}	length of the unused bed, m
m	initial adsorption rate in Elovich equation, kg kg^{-1} s^{-1}
n	Freundlich parameter, -
$\bar{q}$	mean value of the concentration in the particle, kg kg^{-1}
q_b	adsorption capacity in breakthrough point, kg kg^{-1}
q_e	adsorption capacity at equilibrium, kg kg^{-1}
q_i	concentration of the solids at the interface, kg m^{-3}
q_m	Langmuir monolayer capacity, kg kg^{-1}
q_t	adsorption capacity at any time t, kg kg^{-1}
R	gas constant, J mol^{-1} K^{-1}
Re_p	particle Reynolds number, -
r	particle radius, m
Sc	Schmidt number, -
Sh	Sherwood number, -
T	temperature, K
t	time, s
t_b	breakthrough time, s
t_{st}	stoichiometric time, s
u	superficial velocity in the bed, m s^{-1}
u_E	desorption constant in Elovich equation, kg kg^{-1}
$\dot{V}$	volumetric flow rate, m^3 s^{-1}
V_b	effluent volume in breakthrough point, m^3
$\dot{w}$	mass transfer rate in the unit volume of bed, kg m^{-3} s^{-1}
z	location in the column, m
ΔG	Gibbs free energy, J mol^{-1}
ΔH	change in enthalpy, J mol^{-1}
ΔS	change in entropy, J mol^{-1} K^{-1}
ε	porosity of the bed, -

μ_f	viscosity of the fluid, Pa s
ρ_b	density of the bed, kg m^{-3}
ρ_f	density of the fluid, kg m^{-3}
ρ_s	density of the solid, kg m^{-3}

Contents

1 INTRODUCTION

Heavy metals are found in natural waters and especially in industrial effluents. For example copper can cause damage to the brain, liver and some other internal organs. Excessive ingestion of copper can cause vomiting and cramps, or even death [1]. Heavy metals like cadmium and lead tend to accumulate in living organisms and they pose a serious risk for humans and environment. Chronic exposure of cadmium can cause kidney dysfunction and lead can cause central nerve damage. Lead can damage kidney, liver and brain functions [2]. For this reason the level of these pollutants in industrial wastewaters are strictly regulated by authorities and the demand of removing heavy metals from water and wastewater is ever increasing. Some permissible limits for potable water are represented in Table I.

Table I. Word Health Organisation's and EU's drinking water standards for selected heavy metals [3 W].

	WHO, mg/L	EU standard, mg/L
Cadmium	0.003	0.005
Copper	2	2.0
Lead	0.01	0.01

Conventional methods of removing heavy metal from aqueous solutions include chemical precipitation, ion exchange, membrane processes, adsorption and electrochemical treatment technologies etc. [2]. Chemical precipitation is the most widely used in industry but it is inefficient in low concentrations and the disposal of the forming sludge is an issue. Adsorption offers flexibility in design and operation and in many cases it will generate high-quality treated effluent. In addition, adsorbents can be often regenerated and heavy metals can be even recovered. The interest in heavy metal removal by adsorption can be seen from numerous studies aiming to find efficient and inexpensive adsorbent material. The major advantages and disadvantages of the most common heavy metal removal technologies are represented in Table II.

Table II. Conventional heavy metal removal technologies [4, 5]

Method	Disadvantage	Advantage
adsorption	adsorbents require regeneration	flexibility and simplicity of design, ease of operation and insensitivity to toxic chemicals
chemical precipitation	pH dependence difficult separation adverse effect by complexing agent resulting sludges chemicals required	simple and cheap
ion exchange	sensitive to particles high operation cost no selectivity to alkaline metals metallic fouling	pure effluent pure effluent metal recovery possible
membrane	membrane fouling limited life of membrane expensive high pressure	pure effluent
flocculation coagulation	chemicals required (electrolytes)	generate very fine particles of precipitates
flotation	less selective for heavy metals	cost competitive to precipitation
electrodialysis	takes time large electrode surface are required fouling expensive	metal selective

Although adsorption processes are relatively easy to model and design, many methods presented in the literature require simplifying assumptions or need experimental data to be valid. The purpose of this study is to simulate and design an adsorption column for purification of heavy metals from water with an easy method requiring limited amount of information from literature. The study is focused on the removal of Cu^{2+}, Pb^{2+} and Cd^{2+} ions from waters and from wastewaters. Adsorption of heavy metals and suitable adsorbents are discussed in the first part of this paper. Other topics discussed are regeneration of adsorbents and some basic adsorption equilibria and kinetics are introduced. The latter part of

this paper is a case study focused on the simulation and design of adsorption column by using software developed by Reunanen *et al.* [6].

2 ADSORPTION OF HEAVY METALS

In adsorption the molecules distribute themselves between two phases, one of which is a solid and the other is either a liquid or a gas [7]. Due to the nature of heavy metals, only liquid adsorption can be used for heavy metal removal from waters and wastewaters.

2.1 Different types of adsorption mechanisms

Adsorption may be classified as physical adsorption and chemisorption. In the first one the adsorption forces are relatively weak, consisting of mainly van der Waals forces and supplemented in many cases by electrostatic contributions from field gradient-dipole or –quadrople interactions. In chemisorption there is a significant electron transfer, which is equivalent to the formation of a chemical bond between the sorbate and the solid surface. Those interactions are stronger and more specific than in physical adsorption but they are limited to monolayer coverage of the solid surface. Summary of differences between physical adsorption and chemisorption is presented in Table III. [8, 9]

Table III Classifications of adsorption according to [9].

Parameter	Physical adsorption	Chemisorption
heat of adsorption	low, < 1-5 times latent heat of evaporation	high, > 1-5 times latent heat of evaporation
specificity	nonspecific	highly specific
nature of adsorbed phase	monolayer or multilayer, no dissociation of adsorbed species	monolayer only, may involve dissociation
temperature range	only significant at relatively low temperatures	possible over a wide range of temperature
forces of adsorption	no electron transfer, although polarization of sorbate may occur	electron transfer leading to bond formation between sorbate and surface
reversibility	rapid, non-activated, reversible	activated, may be slow and irreversible

2.2 Adsorption mechanisms of heavy metals

Adsorption mechanism varies greatly depending on the adsorbent material and conditions of the adsorption (mainly pH) and adsorbent used. The more detailed discussion of pH is described in later chapters. However, it should be mentioned that heavy metals exist in various forms in water depending on the pH. They are present in aqueous solutions as hexaqua complex ions with six surrounding water molecules [10].

Lyubchik *et al.* [11] suggested that there are different mechanisms for copper adsorption on oxidized and non-oxidized activated carbons. The oxidizing of activated carbon is a chemical treatment to improve the adsorption properties of the adsorbent (in this case, 1M HNO_3 was used). In their study they concluded that the electrostatic interactions (attraction or repulsion) do not seem to have an important effect on the adsorption of the metal on oxidized activated carbons from co-mingled wastes. Mechanism plausible consisted of first fast ion-exchange of the aqueous metal ions (1) and (2), followed by their surface hydrolysis (3) and slower chemisorption and finally outer-sphere complexation that converts inner-sphere complexation with time (4). The latter two reactions could occur in series or parallel. The cation exchange mechanism with carboxylic group is presented in Figure 2. The denotations R_xCOOH represents carboxylic groups (or quinone group) attached in the activated carbon, Me stands for metal.[11]

$$2(-R_xOOH) + Me^{2+} = 2(-R_xOO)Me + 2H^+ \quad (1)$$

$$-R_xOOH + Me(OH)^{1+} = (-R_xOO)MeOH + H^+ \quad (2)$$

$$-[R_xOOH]^- + Me^{2+} \rightarrow [2R_xOO^-Me^{2+}] \quad (3)$$

$$R_xOOH + Me(OH)^{2+} = R_xOOH \ldots Me(OH)^{2+} \rightarrow R_xOO - MeOH^+ + H^+ \quad (4)$$

Kumar *et al*. [12] 2007 postulated that coordination bond formation with amine (-NH_2) group of aniline formaldehyde coated silica gel as the adsorption mechanism. In the presence of mineral acids, the NH_2-group was protonated and good desorption occurred. Barakat [13] investigated adsorption behavior of copper to hydrous TiO_2-adsorbent. Adsorption takes place via the formation of –Cu bonding, like presented in the Figure 1. It was also concluded that this is the main mechanism of hydrous metallic oxide adsorption.

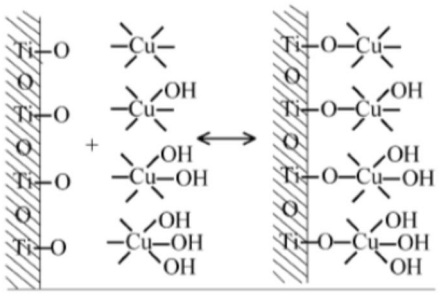

Figure 1. The adsorption mechanism of Cu(II) on hydrous TiO_2. [13]

Barakat [14] reviewed briefly the adsorption mechanisms of modified agriculture and biological wastes (biosorbents) in his study. The adsorption can take place by metabolism-independent metal binding to the external surfaces and cell walls. Adsorption involves ionic, chemical and physical adsorption. Various ligands located on the fungal walls take part in metal chelation. These include carboxyl, hydroxyl, amine, sulfhydryl and phosphate groups. Metal ions are capable of forming complexes with negatively charged reaction sites on the cell wall surface.

Polysaccharide material (modified biopolymers) adsorption mechanism differs greatly from other conventional materials due to its complexity in structure. Biopolymers possess number of different functional groups. Two different mechanisms (chelation versus ion exchange) may involve in metal complexation of chitosan. This is dependent of pH. Chitosan characteristically has many amine groups that are responsible for metal ion binding by chelation. In acidic solutions chitosan is protonated and has electrostatic properties. It can therefore also act as an anion exchanger. Adsorption mechanism in hydrogels is basically governed by

diffusion of water into the hydrogel and the metal ions are trapped inside. This is especially true in the absence of strongly binding sites. [14]

According to Erdem *et al*. [10] adsorption mechanism by natural zeolite is attributed to different mechanisms of ion-exchange processes and adsorption process. Metal ions have to move through channels of the lattice (see Chapter 3.5 for details) and replace the exchangeable cations during the ion-exchange process. The hydrated metal ions were roughly the same size according to measurements, which meant that the exchange may occur via difficulty [10]. This topic was not discussed further in the study, which meant probably that the adsorption mechanism wasn't known in detail. The mechanisms of zeolite adsorption in general differ greatly from other mechanisms.

Figure 2. Cation exchange mechanism with the carbon surface carboxylic group [15].

In some cases it's even possible that precipitation of certain heavy metal may occur and result interesting adsorption behaviors. Turan *et al*. [16] reported that lead precipitated on the surface clinoptilolite (natural zeolite) as lead hydroxide. It was debatable if the precipitation occurred in the surface of the adsorbent or only in the solution because of the poor solubility of lead hydroxide. Precipitation was considered a major lead removal affecting factor in the system.

3 ADSORBENT MATERIALS

An adsorbent, according to Richardson *et al*. [7], has to meet certain requirements in order to be commercially attractive:

- it should have a large internal area.
- the area should be accessible through pore big enough to admit the molecules to be adsorbed. It is a bonus if the pores are also small enough to exclude molecules which it is desired not to adsorb.
- the adsorbent should be capable of being easily regenerated
- the adsorbent should not age rapidly, that is lose its adsorptive capacity through continual recycling.
- the adsorbent should be mechanically strong enough to withstand the bulk handling and vibration that are a feature of any industrial unit.

A practical adsorbent in liquid separation on the other hand has according to Kirk-Othmer [8] four primary requirements: selectivity, capacity, mass transfer rate, and long-term stability. These requirements are discussed below for the most common adsorbents and some newer ones.

3.1 Activated carbon

Activated carbon can be manufactured from naturally occurring carbonaceous materials such as wood, coal, coconut shells or bones decomposed in an inert atmosphere at a temperature of around 800 degrees. The product is not porous and needs additional activation by processes referred as chemical activation or gas activation. [17]

A typical surface area for activated carbon is around 1000 m^2/g [7], although much higher values can be achieved [8], but these very high surface area carbons tend to lack physical strength which hinders their practical use. Activated carbon can be used as powder (PAC) or in granular form (GAC). The granular form is used mostly for gas adsorption and powder is the preferred option for liquid adsorption. Liquid-phase, or decolorizing, carbons are generally fluffy powders with surface area of around 300 m^2/g and the pore size is usually 3.0 nm or larger, which enables faster diffusion [17]. The particle size of granular activated carbon is usually greater than 0.1 mm [18]. In some cases it’s even possible to utilize carbon molecular sieves (CMS) or activated carbon fibers (AFCs) [19], which both have relatively narrow micropore size distribution.

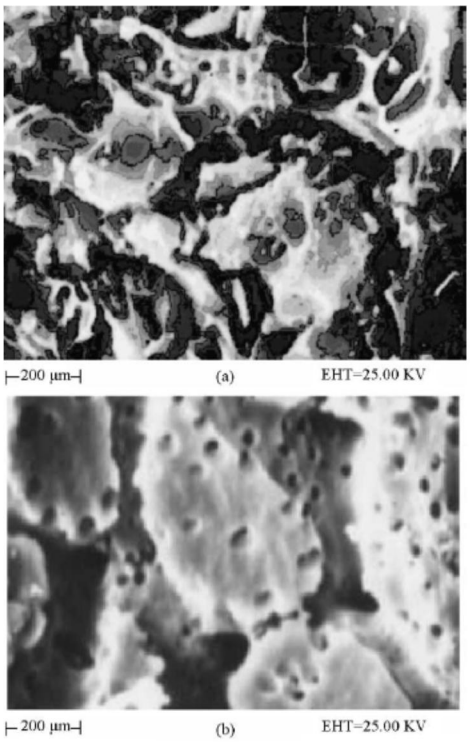

Figure 3. Scanning electron micrograph (SEM) of activated carbon (a) before (b) after treatment [20].

To name some studies, Uzun and Güzel [21] have studied adsorption of some heavy metal ions from aqueous solution by activated carbon and Marinkovski *et al.* [22] concentrated their studies on granular activated carbon (adsorption capacity for Cd^{2+} and Pb^{2+}, 20.1 and 17.9 mg/g; respectively). An *et al.* [23] obtained adsorption capacities for Pb^{2+}, Cu^{2+} and Cd^{2+} ions for several adsorbents. Adsorption capacities were for PAC 26.9, 4.4 and 3.4 mg/g and for GAC 16.6, 5.1 and 3.4 mg/g; respectively. Dwivedi *et al.* [18] got similar results for GAC for Pb^{2+} with adsorption capacity of 26.5 mg/g. Leyva-Ramos *et al.* [24] investigated adsorption of Pb^{2+} on various types of activated carbon fibers and received the best adsorption capacity of 36.6 mg/g. Due to the relative expensiveness of activated carbon there are a lot of studies trying to manufacture a cheap adsorbent materials. Lyubchik *et al.* [11] are one of them by converting waste into activated carbon and studying heavy metal removal from wastewater. Goel *et al.* [20] are one of the many to investigate the modifications of activated carbon (granular). The properties of unmodified and modified were studied. The treated activated

carbon showed 35% increase in uptake capacity of lead ions. The surface of the activated carbon before and after treatment is shown in Figure 3.

3.2 Silica gel and hydrogels

Pure silica, SiO_2, is a chemically inactive non-polar material but when it has a hydroxyl group (silanol group), its surface becomes very polar and hydrophilic. The surface area of silica gel varies from 100 to over 800 m^2/g. The product is provided in granular and spherical forms. Pore sizes are typically from 2.0 - 16 nm [17]. Due the silica-gel surface has an affinity for water and organics, the primary adsorptive application of silica gel is the dehydration of gases and liquids. Silica gel doesn't belong to the most attractive heavy metal removal adsorbents and there aren't many recent studies. Tran and Roddick [25] investigated adsorption of lead ions on fixed beds with silica gel and the use of silica gel as carrier have occurred in many studies, such as Kumar *et al.* [12] research of uptake and desorption of copper ion using functionalized polymer coated silica gel in aqueous environment. The obtained adsorption capacity for Cu(II) was 76.3 mg/g.

According to Lyubchik *et al*. [26] Hydrogels are polymeric materials having carboxylic acid, amide, amine or ammonium groups which can bind heavy metal ions. Hydrogels tend to swell by the ionic strength, pH and temperature the same way as silica gel does. Figure 4 shows a schematic representation of polymerization and crosslinking reaction. It results a three-dimensional network formation of cationic hydrogel. The main problem with these adsorbents is their durability, which is not at the level of commercialization.

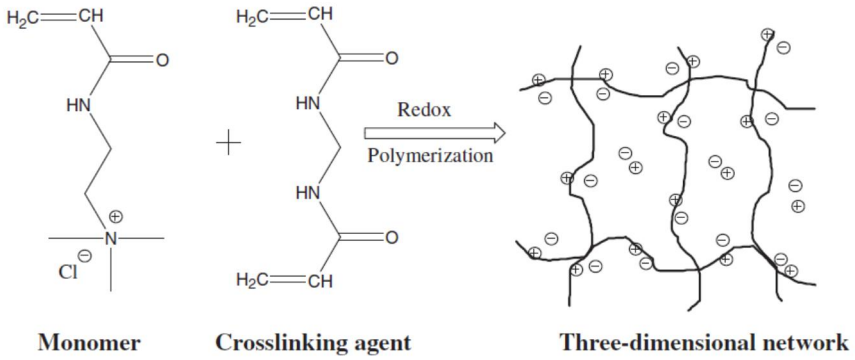

Figure 4. Three-dimensional formation of cationic hydrogel. [26]

Krusic *et al.* [27] studied poly(acrylamide-co-sodium methacrylate) hydrogels for Pb^{2+} adsorption (adsorption capacity 68.9 mg/g). Wang *et al.* [28] researched poly(polyethylene glycol diacrylate) and poly(methylacrylic acid) adsorbents. Adsorption capacities for Pb(II), Cu(II) and Cd(II): 114.0, 22.9, 37.1 and 466.2, 78.8, 121.4 mg/g, respectively, were obtained. Wang *et al.* [29] compared adsorption capacity of new hyper-crosslinked polystyrene adsorbent to two commercial adsorbents. The new sorbent achieved capacity of Cu^{2+} removal of 126.6 mg/g, which was noticeably higher than the commercial ones.

3.3 Activated alumina

Aluminum oxides have several crystal forms. Activated alumina that is used as adsorbent is mainly γ-alumina. Porous alumina is produced by dehydration of alumina hydrates. Typical specific surface areas range from 200 to 500 m^2/g and the predominant pore diameter is in the 2 - 5 nm range. Activated alumina cannot compete in terms of capacity and selectivity to for example molecular sieve zeolites. One of the biggest assets is the durability of the material and activeated alumina is widely used in moving-bed applications. The most important industrial applications are found in drying processes for both liquids and gases. [17]

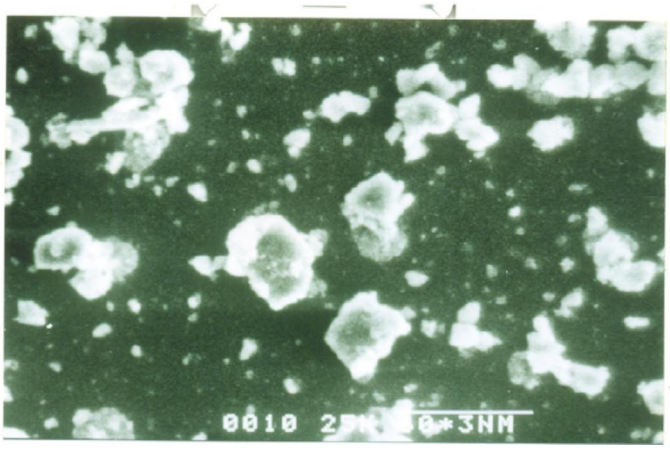

Figure 5. Scanning electron micrographs (SEM) of activated alumina (500x). [30]

Liu *et al*. [31] conducted a study of adsorption of copper(II) and chromium(IV) on diaspora, which is a naturally occurring aluminum oxide. Adsorption capacity of 1.9 mg/g for copper ions was achieved. Activated alumina was the subject of the study by Naiya *et al*. [30] (surface of the adsorbent shown in Figure 5) and they obtained adsorption capacities of 35.1 and 83.3 mg/g for Cd(II) and Pb(II), respectively.

3.4 Nanosized metallic oxides

Most widely studied nanosized metal oxides (NMOs) for heavy metal removal include aluminum, iron, manganese and titanium oxides. The size and shape of NMOs varies and they are both important factors affecting adsorption performance. Particle size of NMOs vary from 2 to several hundreds of nanometers (latter number for needlelike particles) and surface area is in the range of 25 – 400 m^2/g. NMOs provide an effective and specific heavy metal adsorption. They exist as fine or ultrafine particles, which causes problems due to agglomeration, difficult separation and excessive pressure-drops when used in flow-through systems. To overcome these problems there is a lot of research going on in the field of manufacturing NMOs and fabricating them by impregnating or coating NMOs particles into porous supports of larger size. These supports include natural hosts such as bentonite and sand, metallic oxide materials, such as Al_2O_3 membrane, and porous manganese oxide complex and synthetic polymer hosts, such as cross-linked ion-exchange resins. However the use and

fabrication of NMOs is still in development stage and various issues needs to be solved before commercial use. [32]

Hua *et al.* [32] listed some typical values for heavy metal removal with nanosized metallic oxides. For lead ions the values varied from 9.2 to 324.3 mg/g (the highest for hydrous manganese oxide), for copper ions values ranged from 15.4 to 1600 mg/g (the highest value for zinc oxide) and for cadmium ions values ranged from 7.9 to 143.3 mg/g (hydrous manganese oxide as the top value).

3.5 Zeolites and clay

Zeolite is an aluminosilicate mineral which is formed in hydrothermal conditions. Zeolites can be found naturally but they can also be produced industrially. More than 40 kinds of zeolite have been found in natural mines but oddly more than 150 different types can be made synthetically. [17]

Because of the regular crystalline structure, zeolites provide unique adsorption characteristics and adsorbents with very narrow pore size distribution are possible. The adsorption takes places within the crystals, in which the access is limited by the pore size. Zeolites can therefore selectively adsorb or reject molecules based on their molecular size which is called the molecular-sieve effect. The adsorption in zeolites cannot be explained with traditional theories of adsorption. [17]

An *et al.* [23] compared several adsorbents in their study relating adsorption capability of crab shells. They got heavy metal uptakes of zeolite for Pb, Cu and Cd: 111.9, 14.6 and 30.4 mg/g; respectively. Erdem *et al.* [10] investigated removal of heavy metal cations by natural zeolites and got a result of 9.0 mg/g adsorption capacity for Cu(II) removal with natural zeolite. Marinkovski *et al.* [22] obtained adsorption capacities for natural zeolite for Cd^{2+} and Pb^{2+} with results of 18.4 and 18.7 mg/g, respectively.

Clay minerals are being studied for heavy metal removal. There are three different types of clay: montromorillonite, bentonite and kaolinite. Among clay minerals the first two have shown reasonable removal for Cu(II). Compared with adsorbents from agricultural wastes, the price of these materials is relatively higher. [33]

Kurniawan *et al.* [33] reported several heavy metal uptakes by unmodified and modified natural materials, some of which are listed in the Table IV.

Table IV. Some adsorption capacities of heavy metals on natural materials. [33]

Adsorption material	Adsorption capacity of Cu^{2+}, mg/g	Adsorption capacity of Cd^{2+}, mg/g
Natural zeolite	25.04	-
HCl treated clay	83.3	-
Kaolinite	1.9 - 10.79	0.75 - 4.47
Modified kaolinite	4.8	8.6
Ball clay	3.0	2.24
Bentonite	9.27	18.16
Diatomite	3.24	5.54
Montmorillonite	3.04	5.20

Gupta and Bhattacharyya [34] studied 6 different kind of clays with modifications and they obtained adsorption capacities between 9.0 to 31.4 mg/g for Pb(II). The value for unmodified clay was 11.5 mg/g. Bhattacharyya and Gupta and [35] got adsorption capacities (in the same conditions and with same adsorbents as the study mentioned earlier) between 3.0 to 28.8 mg/g for Cu(II).

3.6 Biosorbents

According to Cho *et al*. [4] biosorption is a process that utilizes dead biomass to remove toxic heavy metals. Biosorbents are prepared from waste biomass of industry or from suitable natural sources. One special case of this is use of microbial biomass such as different types of bacteria, algae and fungi. The binding capacities of some biomass can be compared with the commercial cation exchange resins. The biosorption has not been commercialized, although the research has been extensive for decades according to Wang and Chen [36]. The writers were skeptical if the biosorbents would have any competition in many types of industrial scale metal removal applications.

Singht *et al*. [37] studied use of filamentous algea *Pithopora oedogonia* for Cu(II) and Pb(II) removal from aqueous solution with adsorption capacities of 23.1 and 71.1 mg/g, respectively. The results were compared with some other biosorbent studies. Adsorption capacities for Cu(II) were 18.8 – 23.3 mg/g with unicellular algea, 29.3 mg/g with seaweed and 8.7 – 133.3 mg/g with other filamentous algae. Comparison to lead ions removal uptakes were 97.4 mg/g for unicellular algae, 54.0 – 229.0 mg/g for seaweeds and 31.1 – 198.5 mg/g for filamentous algae.

3.7 Industrial wastes

Some industrial wastes such as fly ash, blast furnace slag and sludge, red mud, lignin and waste slurry etc. are currently being researched as potential low-cost adsorbents to remove heavy metal from wastewater. Ahmaruzzaman [5] conducted a study on these low-cost adsorbents and found out that modified industrial wastes showed high adsorption capacities. It was concluded that removal of heavy metals with industrial wastes as adsorbents poses few drawbacks similar to biosorbents, such as lack of study on utilization of them in commercial scale. The review indicated need for further study on several aspects such as column studies, regeneration and adsorption mechanisms in detail [5]. Kurniawan *et al.* [33] published a comparison of low-cost adsorbents for treating wastewaters laden with heavy metals and it was evident that adsorbents from industrial waste demonstrate outstanding capabilities for the removal of heavy metals. Some adsorption capacities of industrial wastes are presented in Table V. Technical applicability and cost-effectiveness were said to be the key factors for selection of the most suitable adsorbent.

Table V. Some adsorption capacities of industrial by-products or wastes [33].

Adsorbent material	Adsorption capacity of Cu^{2+}, mg/g	Adsorption capacity of Cd^{2+}, mg/g	Adsorption capacity of Pb^{2+}, mg/g
Waste slurry	20.97	15.76	1030
Red mud	106.44	66.67	-
Lignin	6.7 – 22.87	6.7 - 25.40	8.2 – 1865

4 REGENERATION OF ADSORBENTS

Loaded adsorbents can be regenerated by temperature- or pressure-swing processes [38], but this is not the case with heavy metals. Other methods are displacement and extraction. Acid solutions are the preferred desorption agent to desorb heavy metal ions from the adsorbent.

Wang *et al.* [29] used 2% HCl (hyper-crosslinked polystyrene adsorbent, Cu^{2+}), which effectively desorped the adsorbent. The cycle was repeated for 5 times with desorption efficiencies varying from 93.3 to 96.8% and the breakthrough time decreased insignificantly. Gupta *et al.* [39] used 3M HNO_3 (activated carbon from fertilizer waste, Pb^{2+}) with 88% recovery in the first desorption cycle. However, the adsorption capacity declined almost 50% until the end of the sixth regeneration cycle. Singh *et al.* [40] conducted five sorption-desorption cycles using 0.1 M HCl (*Pithophora* biomass, Cu^{2+} and Pb^{2+}). The adsorption decreased 41% for Cu(II) and 25% for Pb(II) removal. The results are shown in Figure 6 and they were average compared to some other studies with biosorbents. Biomass loss of 10 - 15% was recorded at the end of the regeneration cycles. Krusic *et al.* [27] used 0,01 M HNO_3 (hydrogel, Pb^{2+}) and their desorption studies suggested that the adsorption was realized mainly by electrostatic attraction. The adsorption capacity did not show significant changes after multiple recycles. Wang *et al.* [28] got promising results for hydrogel desorption. Desorption was higher than 96% and after three cycles, desorption rate did not alter significantly.

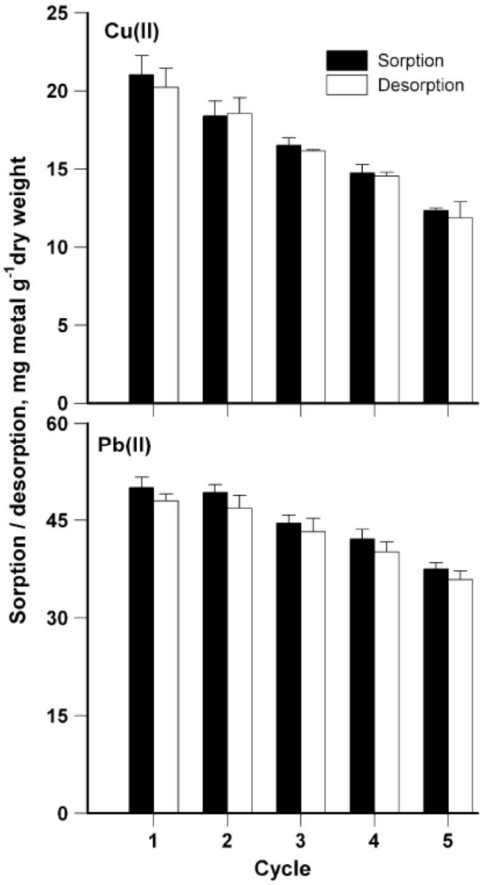

Figure 6. A typical results for regeneration study: Adsorption and desorption cycles of Cu(II) and Pb(II) by *Pithopohora*. Adsorption initial concentration 100 mg/L, temperature 25°C, time 30 min, biomass concentration 1 g/L. 0.1 M HCl was used as desorbing agent [40].

Kumar *et al.* [12] studied desorption more widely on functionalized polymer coated silaca gel. Desorption of copper ions was carried out by using four types of desorbents (HCl, H_2SO_4, HNO_3, EDTA). The equilibrium was achieved in 40 minutes in the batch study. 0.2 M HCl resulted 72% and 0.002 M EDTA resulted 62% of maximum desorption. With 1 M mineral acids and 0.2 M EDTA desorption efficiencies were all in the range of 97 - 100%. The removal of heavy metals from adsorbent was claimed to be due to the protonation of amine groups. Granular activated carbon in packed bed column was studied for Pb(II) removal by Dwivedi *et al.* [18]. Use of high concentration nitric acid was addressed to provide better results for desorption because the high concentration of HNO_3 equals to higher quantity of exchangeable H^+ ions. However, in actual elution process, it may result serious problems occurred in the disposal of the highly

acidic effluent. For this reason the desorption studies were conducted with 0.5 M HNO_3.

Column studies differ from batch studies: in batch studies, the system reaches equilibrium in the flask, whereas in the column the fresh eluent is fed to the column continuously. An example of desorption in column is presented in Figure 7. At first the effluent concentration increased rapidly, until it starts to decline and, in this case, desorption was negligible after 1 hour. In columns the amount of desorbing agent is often optimized and like in the study by Kumar and Bandyuopadhyay [41] the column was operated in counter-current mode (opposite direction of adsorption). The flow rate was also decreased slightly to improve desorption economy.

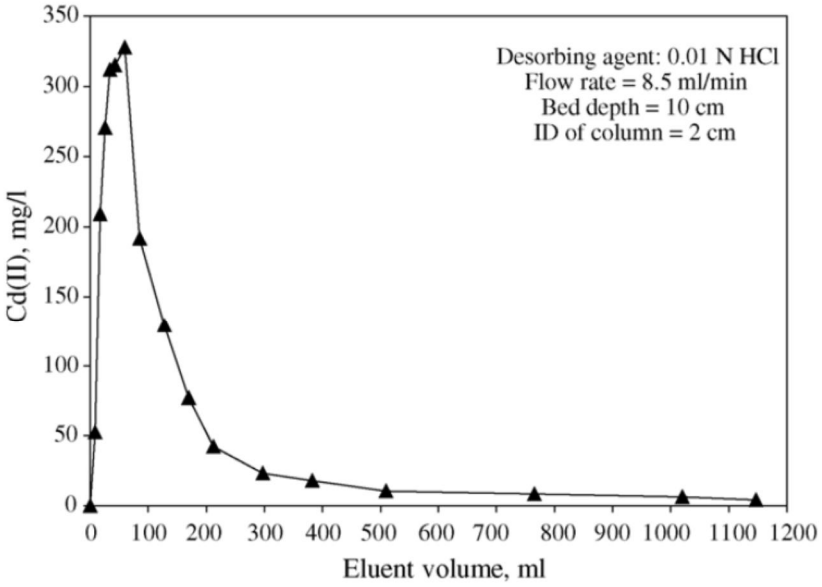

Fig. 9. First cycle desorption profile of Cd(II).

Figure 7. Desorption of Cd(II) from treated rice husk [41].

Desorption studies can reveal a lot from the adsorption mechanism of studied adsorbent. In some cases it is possible, for example, to get information of the percentage of chemical adsorption versus physical adsorption with the aid of adsorption and desorption studies. [12]

In some cases the regeneration may give better results for adsorption for at least during the first couple of desorption cycles. For example this was observed in the regeneration study by Katsou *et al.* [42] with natural zeolite. Multiple reasons were speculated: removal of impurities from channels of zeolite, modification of used KCl solution by replacing ions originally in the material, formation of complexes among chlorides and metals.

5 ADSORPTION EQUILIBRIA

The adsorption equilibrium is the phenomenon when the rate which molecules are adsorbed is equal to the rate of which they are desorbed. There are many theories to describe the phenomena but none of them fully explain the physical and chemical effects occurring in adsorption. Fortunately, for engineers it is not relevant to know all the details in order to calculate the process in a satisfactory level. For this reason most of the theories developed in earlier stages are still very useful, although some of the assumptions in them are not entirely valid. Most of the theories are developed for gas-adsorption mainly because the gaseous state is better understood than liquid. Part of this behavior is explained by the lack of industrial applications in liquid processes. [7]

The adsorption equilibrium is described mainly by the relation between the concentration of a component in the fluid phase and its loading on the adsorbent. For liquid adsorption of heavy metals, the amount of component in the fluid is normally expressed as a molar or mass concentration (moles per liter or grams per liter). The absorbent loading is represented either by mass loading (milligrams of adsorbate per gram of adsorbent) or mole loading (moles of adsorbate per grams of adsorbent). The most common way to represent adsorption equilibrium is to keep the temperature constant and plot concentration of metal ion at equilibrium C_e against adsorption capacity in equilibrium q_e to give an adsorption isotherm. An example is presented in Figure 8. Other possibilities are for instance keeping C_e constant gives adsorption isostere. In gas-liquid systems the pressure can be kept constant to obtain adsorption isobar. [7]

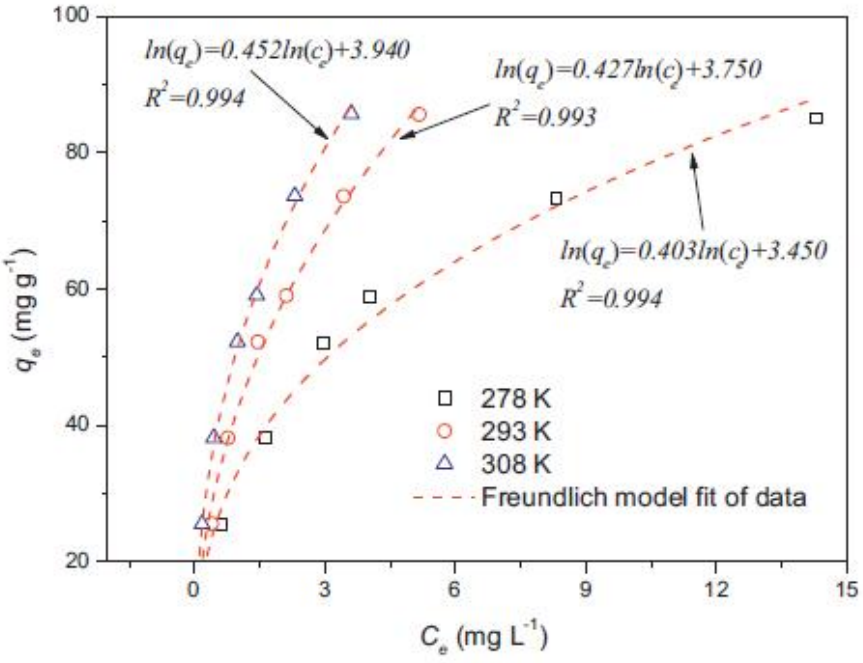

Figure 8. Adsorption isotherms of Cu^{2+} on WJN-101 (new cross-linked polystyrene adsorbent) at different temperatures [29].

5. 1 Adsorption isotherms for single-component equilibria

Singe-component adsorption isotherms can be generally characterized by some typical curves (I-V), which are shown in Figure 9. The type I is the most favorable and the type III is unfavorable. It should be noted that some of these types do not exist in liquid adsorption systems. These isotherms are often described by some equations presented in the following chapters.

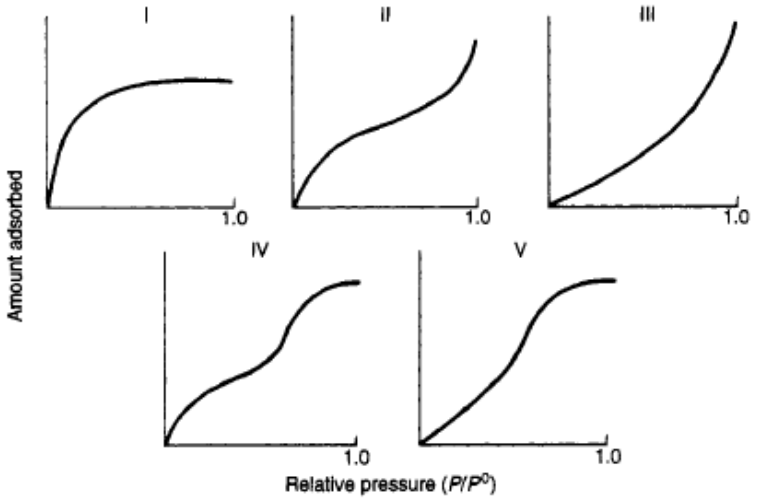

Figure 9. Classification of isotherms into five types according to Brauner, Deming, Deming and Teller [7].

5.1.1 Freundlich adsorption equation

The Freundlich adsorption equation is one of the most used mathematical expressions to describe an adsorption system. It is expressed as

$$q_e = K_f C_e^{(1/n)} \tag{5}$$

where q_e adsorption capacity at equilibrium

K_f Freundlich constant

n dimensionless Freundlich parameter

C_e equilibrium constant of solute.

To linearize the data, the Freundlich equation is written in mathematical form

$$\log q_e = \log K_f + \frac{1}{n} \log C_e \tag{6}$$

K_f describes Freundlich adsorption capacity and the dimensionless exponent n denotes the favorability of adsorption ($0<n<10$ favorable).

5.1.2 Langmuir adsorption equation

The Langmuir adsorption equation is described by equation

$$q_e = K_a q_m c_e/(1 + K_a c_e) \quad (7)$$

where K_a Langmuir constant

q_m Langmuir monolayer capacity.

Equation (7) assumes that rate of adsorption is proportional to the empty surface available as well as to the fluid concentrations. The equation is valid until monomolecular coverage and it assumes that there are no interactions between the molecules on the surface and the energy of adsorption is the same all over the surface.

Although the model assumptions, it can be used for situation where the assumptions are not valid. The equation is probably the most used adsorption isotherm in liquid adsorption of heavy metals. Typical adsorption isotherms for the selected heavy metal removal are presented in Figure 10.

Dimensionless separation factor (known as constant separation factor or equilibrium parameter) R_L describes the favorability of the adsorption:

$$R_L = (1 + K_a c_0)^{-1} \quad (8)$$

where c_0 concentration of initial metal ion solution.

Values between $0 < R_L < 1$ indicate favorable reaction process, $R_L = 0$ irreversible case, $R_L = 1$ linear case and $R > 1$ unfavorable reaction. [43]

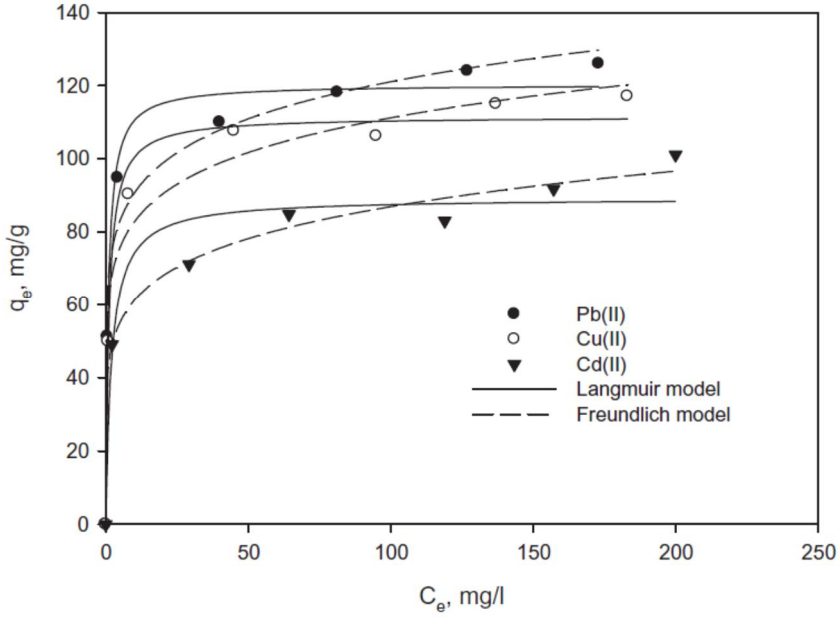

Figure 10. Adsorption isotherm of Pb(II), Cu(II) and Cd(II) on MDA-SBA-15 (a) Langmuir and (b) Freundlich at the adsorbent dose of 1 g/L, pH 4.0 and temperature of 25°C [44].

5.1.3 Redlich-Peterson model

Redlich-Peterson model (R-P) [45] is presented (according to [46]) in the form:

$$q_e = \frac{Ac_e}{1+Bc_e^g} \tag{9}$$

where A, B R-P model constants

g dimensionless R-P parameter.

The parameter g should be in the range of 0 to 1.0. For g = 0 and g = 1, the equation is analogous to Henry's law and to Langmuir equation, respectively.

5.1.4 BET equation

Another common adsorption equation was presented by Brauner, Emmet and Teller (BET) [47]. The equation is written in form (according to [46]):

$$q_e = \frac{q_s C_{BET} c_e}{(c_s - c_e)[1+(C_{BET}-1)(c_e/c_s)} \quad (10)$$

where c_{ML} adsorbate monolayer saturation concentration

C_{BET} BET adsorption isotherm constant

q_{s} theoretical adsorption isotherm capacity.

The details of the validity of this equation are not discussed here. However, it can be used to describe multilayer sorption and it can represent all the five types of adsorption isotherms.

5.1.5 Other adsorption isotherms

In the literature there are several other ways to describe single component adsorption isotherms. Ahmaruzzamann [5] has listed several cases used in articles for single and multicomponent adsorption models reported in the literature. For single-component adsorption there are also Sips Isotherm, Radke-Prausnitz, Frenkel-Halsey-Hill (FHH), Tempkin, Toth, Flory-Huggins, Koble-Corrigan, MacMillan-Teller (MET), Dubinin-Radushkevich and Khan isotherm types.

5.2 Adsorption kinetics

5.2.1 Modeling adsorption

The kinetics of adsorption may be controlled by several independent phenomena. These can work in series or parallel and they often fall in one of the following general categories: bulk diffusion, external mass transfer (film diffusion), chemical reaction (chemisorption) and intraparticle diffusion (pore diffusion). Several kinetic analyses are being applied to adsorption and not only they express the adsorption rates but also give indications of possible adsorption mechanisms. [48]

5.2 Kinetics model used

Several simplified kinetics models are being used in researches. The most widely used are presented in the following chapters [46]. An example of a kinetic study is shown in Figure 11.

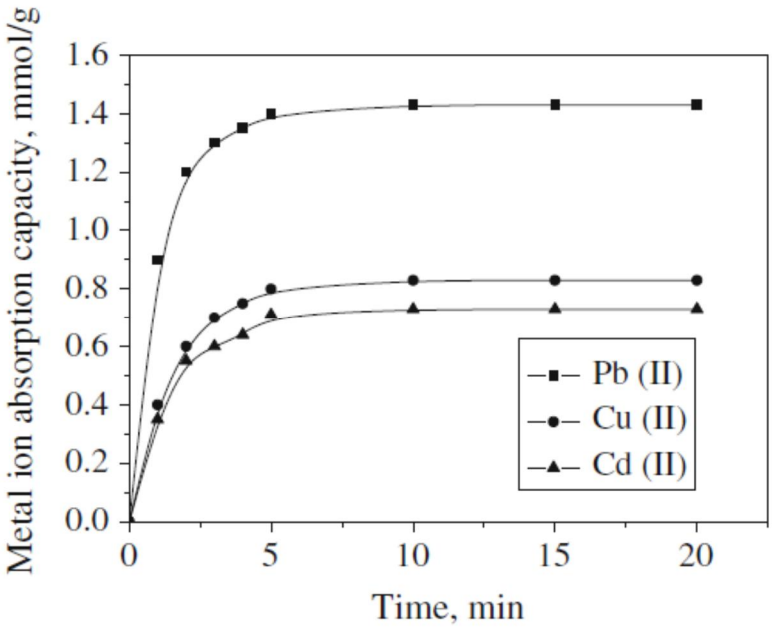

Figure 11. Results of adsorption studies of Pb(II), Cu(II) and Cd(II) on hydrogel [28].

5.2.1 Pseudo-first order kinetic model

The pseudo-first order kinetic model was presented by Lagergren [49]

$$q_t = q_e[1 - \exp(-k_1 t)] \tag{11}$$

where q_t adsorption capacity at any time t

k_1 pseudo-first order diffusion rate constant

t time.

5.2.2 Pseudo-second order kinetic model

The pseudo-second order kinetic model is described by the following equation [50]

$$q_t = \frac{t}{(1/k_2 q_e^2) + (t/q_e)} \tag{12}$$

where k_2 pseudo-second order rate constant.

Parameters for this equation can be derived by plotting t/q_t against t. This model has been applied widely in the recent years to the adsorption of pollutants from wastewaters. The equation fitted to experimental batch operation data very well in large quantity of literature reported according to Ahmaruzzaman [5]. The rate expression is used to describe chemisorption. The main advantages of using pseudo-second order equation are that the initial rate of the adsorption and equilibrium concentration can be obtained from the model.

5.2.3 Intraparticle diffusion kinetic model

The intraparticle diffusion kinetic model was presented by Weber and Morris [51]

$$q_t = k_{id} t^{0,5} + C_{id} \quad (13)$$

where k_{id} intra-particle diffusion rate constant

C_{id} parameter.

C_{id} represents external convective mass transfer from the bulk liquid to the surface of the solid as it has same unit with q_t, which gives an idea of the thickness of the boundary layer (the greater the C_{id} the greater is the boundary layer effect).

These parameters are obtained by fitting q_t against square root of time. If a good fit is obtained and if the plot passes through origin (C_{id} = 0), then according to Weber and Morris, the intra-particle diffusion is the rate limiting step. But if the plot yields multi-linear proportions, there are several rate limiting steps in the adsorption.

5.2.4 Elovich equation

The Elovich equation [52] is presented by equation (14)

$$q_t = u_E \ln(m u_E) + u_E \ln(t) \quad (14)$$

where u_E desorption constant

m initial adsorption rate

q_t amount of metal removed at time t

The Elovich equation parameters m and u can be obtained by plotting q_t against $\ln(t)$. The equation is useful for determining the initial adsorption rate.

In general it should be noted that analysis of results from different kinetics models is somewhat neglected in many studies.

5.3 Breakthrough curve

Fixed-bed columns are used in the majority of large-scale applications of the adsorption processes. The behavior of fixed-bed column is often illustrated with breakthrough curves, like presented in the Figure 12. Adsorbent material is packed in a column and fluid flows continuously through the column where dynamic adsorption takes place. As the process continues, the amount adsorbed on top of the column becomes in equilibrium with the adsorbate influent concentration. This is called the saturation zone. Thereafter can be observed a region with increasing concentration of the adsorbate in which the mass transfer occurs, also called as the mass transfer zone (MTZ), or sometimes referred as the shock wave front. The depth of this zone is controlled by many variables such as characteristics of the adsorbate and the adsorbent, flow velocities and bed height. This zone advances to the bottom of the column where the adsorbate concentration in the fluid starts to rise gradually. This breakthrough point eventually turns into exhaustion point. Normally the breakthrough curve takes an S-shape. Systems with high film transfer coefficients, high internal diffusivities or favorable isotherms result steeper slopes. [18]

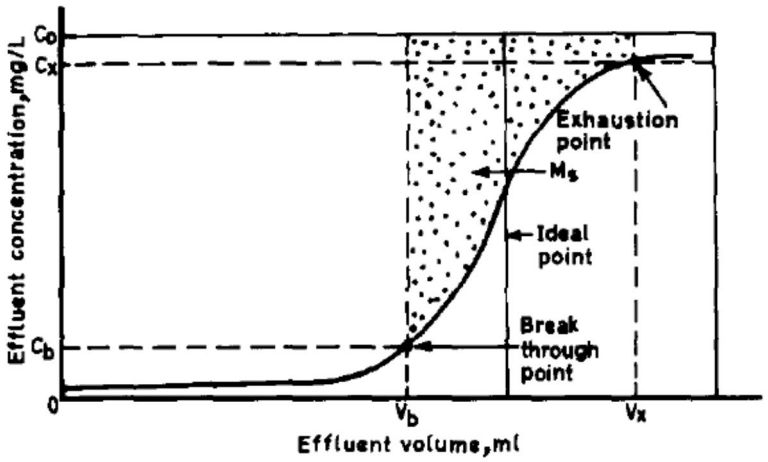

Figure 12. Idealized breakthrough curve [39].

It should be noted that the effluent contains always some amounts of adsorbate and the theoretical equilibrium concentrations is rarely achieved in real situations. Term minimal effluent concentration is defined as the average concentration of the metal ion in the effluent at the initial constant phase [20].

The mass transfer resistance and the axial mixing in real systems lead to deviations from the equilibrium theory. In systems with favorable isotherms the shock wave front is replaced by a term called constant pattern behavior. The concentration profile spreads in the initial region until stable situation is achieved. At this point the mass transfer occurs at the same rate at every point along the wave front. This means that the shape of the mass transfer zone remains unaltered for majority of the bed. [8]

6 FACTORS AFFECTING ADSORBTION EQUILIBRIA

It is absolutely crucial to recognize that the adsorption equilibria is a very complicated phenomena. The adsorption capacities of the adsorbnets presented in this study are only strong indications of the uptakes and they can differ substantially in different conditions.

6.1 Effect of pH

According to Kocaoba *et al.* [53] it is generally accepted that adsorption of heavy metals increases by increasing the pH value. Most of the heavy metals form precipitates at pH higher than 6 and results of adsorption studies are no longer

reliable. Ahmaruzzaman [5] reported on industrial wastes as adsorbents that in certain pH range most metal adsorption increases with increasing pH up to a certain value. This can be explained with changes in the surface charge of the adsorbent and the metal species with changing pH values. When both of these surface charges become negative, the adsorption will decrease significantly. This is not the case for some heavy metals that exist as negative ions in solutions, such as chromium. Chromium may release hydroxide (OH^-) instead of proton (H^+) when adsorbed in certain materials.

It is known that cupper exists in various forms in an aqueous environment. Those forms are Cu^{2+}, $CuOH^+$, $Cu(OH)_2^0$, $Cu(OH)^{3-}$ and $CU(OH)_4^{2-}$ as shown in the following equations

$$Cu(OH)_{2(s)} \leftrightarrow Cu^{2+} + 2OH^- \quad (15)$$

$$Cu^{2+} + OH^- \leftrightarrow CuOH^+ \quad (16)$$

$$CuOH^+ + OH^- \leftrightarrow Cu(OH)_{2(aq)} \quad (17)$$

$$Cu(OH)_{2(aq)} + OH^- \leftrightarrow Cu(OH)_3^- \quad (18)$$

$$Cu(OH)_3^- + OH^- \leftrightarrow Cu(OH)_4^{2-} \quad (19)$$

Within pH 3 - 6 Cu^{2+} is the most dominant species in the solution while if the pH is above 6, the $Cu(OH)_{2(s)}$ starts to precipitate, depending on the concentration of solution (for example, 100 mg/L solution: the precipitation point is at pH 6.10).

Kumar *et al.* [12] reported that increasing pH resulted better adsorption capacities of Cu for aniline formaldehyde coated silica gel. At initial concentration of 100 mg/L, the capacities rise from 5.8 mg/g to 20.4 mg/g when pH increased from 5.4 to 6.0.

Krusic *et al*. [27] removed lead ions for water by poly(acrylamide-co-sodium methacrylate) (AAm/SMA) hydrogels and investigated effect of pH in the range 2.0 – 6.0. At pH 5 the solubility of $Pb(OH)_2$ is high and Pb^{2+} ions are the main species in the solution. The pH higher than 6 was not investigated to avoid precipitation of Pb. The adsorption capacity increased with increasing pH; reaching the optimal value at pH 5.0, as indicated in the Figure 13.

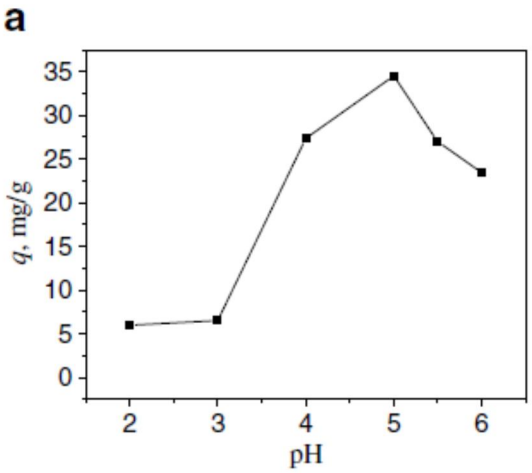

Figure 13. The effect of pH on adsorption capacity of Pb2+ ions onto AAm/SMA hydrogels. [27]

Kurniawan *et al*. [33] noted that activated carbon performs efficiently at acidic pH range (2.5 to 7.0) and has the ability to treat wastewaters with metal concentration ranging from to 10 to 1000 mg/L.

Bhattacharyya and Gupta [35] reported that the number of available hydrogen ions is high at low pH. Cu^{2+} ions have to compete with them for the adsorption sites, which are weakly acidic in nature. Thus increasing pH, the active sites become gradually deprotonated and favor more and more Cu^{2+} uptake. According to Bhattacharya and Gupta [35], similar behavior has been reported by various other authors.

6.2 Effect of initial metal ion concentration

Generally the adsorption uptake rate is increased with increasing metal concentration of the heavy metals. Overcoming the mass transfer limitations is the primary reason for this behavior [5]. Erdem *et al*. [10] claimed that metal adsorption removal percentage decreases with increasing metal concentration by natural zeolite (the studied heavy metals were Cu, Co, Zn and Mn). This was an indication of that less energetically favorable sites take part in the adsorption mechanism. For example the adsorption percentage for copper ions decreased from over 65% to a slightly over 20% when the initial metal concentration was increased from 100 to 400 mg/L.

Dwivedi *et al*. [18] investigated the effect of initial lead ion concentration to breakthrough curve shapes in their column studies for Pb2+ removal. They found out that the larger the initial concentration, the steeper is the slope breakthrough curve and the time to reach breakthrough time is smaller. This is shown in the Figure 14. The diffusion process is concentration dependent and as the initial metal concentration increases, the metal loading rate increases. In the same time the driving force of the mass transfer increases, which results decrease in the adsorption zone length (steeper slope).

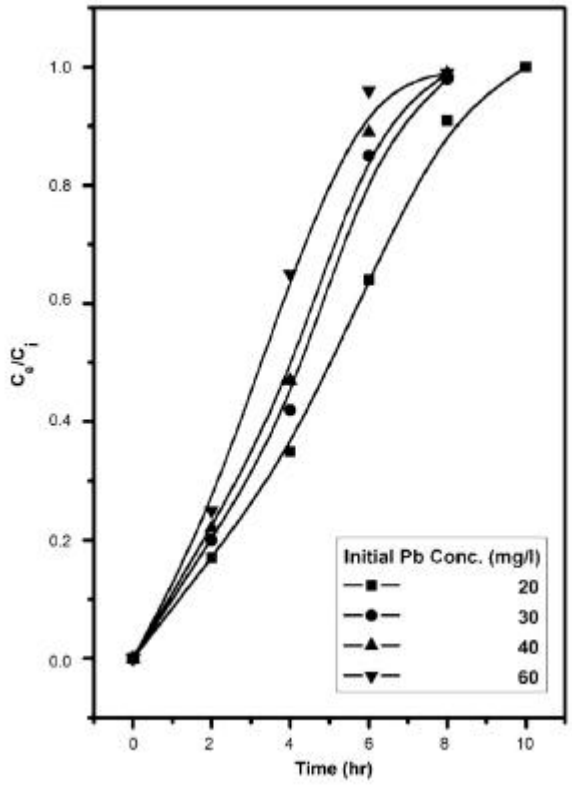

Figure 14. Breakthrough curve for different feed concentrations at constant hydraulic loading rate of 12 $m^3/(h\ m^2)$ with granular activated carbon adsorbent. [18]

6.3 Effect of temperature

The majority of the conducted studies in the literature lack the temperature dependency studies. One probable reason for this is the fixed temperature of many applications (industrial effluents etc.). However, temperature dependency studies reveal a lot from the mechanism and the nature of the adsorption. Thermodynamic parameters like Gibbs free energy, entropy and enthalpy can be obtained from from isosteric experiments (q_e is calculated from adsorption isotherms at different temperatures and q_e is kept as constant) using equation (20). [54]

$$lnK_d = {\Delta S}/{R} + {\Delta H}/{RT} \quad (20)$$

where K_d distribution coefficient of the adsorbate (q_e/c_e)

ΔS change in entropy

ΔH change in enthalpy.

Thermodynamic parameters are calculated by plotting ln(K_d) versus 1/T. The values for Gibbs energy can be computed from the Gibbs relation (21):

$$\Delta G = \Delta H - T\Delta S \quad (21)$$

where ΔG Gibbs free energy.

When deriving the values of thermodynamic properties, it is assumed that the enthalpy doesn't change with temperature.

The dominant trend seems to be that the uptake of heavy metals from water rises with increasing temperature. Typical result for temperature dependency study is presented in the Figure 15.

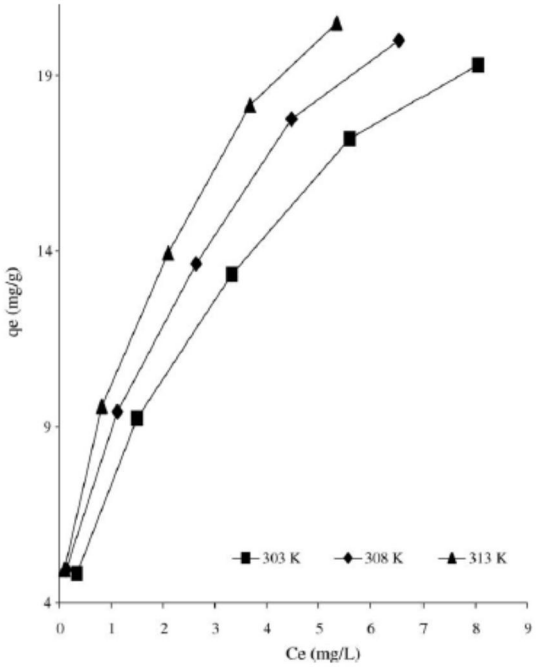

Figure 15. Adsorption of copper ions to montmorillonite (clay 2 g/L; initial Cu(II) concentration 10, 20, 30, 40, 50 mg/L; pH 5.7; time 360 min) [35].

Bhattacharyya and Gupta [35] concluded that adsorption of Cu^{2+} on clay increases with increasing temperature, as shown in Figure 15. First possibility is that the copper ions overcome the activation energy of attaching to the surface more readily in higher temperatures. The second possibility arises from dissociation of the surface components of clay created by the additional adsorption sites. Endothermic adsorption was suggested although thermodynamic data in other sources was rather scarce and didn't fully match the case.

Krusic *et al*. [27] found that increase in temperature from 25 °C to 45 °C, adsorption capacity increased slightly for AAm/SMA hydrogel removal of lead ions. This was attributed to higher swelling (increase in porosity, total volume and active sites in the adsorbent) and decrease in the boundary layer thickness of the sorbent. Kocaoba [55] observed also only slight improvement in adsorption capacity (temperature range 20 – 60 °C) with Pb(II) and Cd(II) removal by dolomite. The adsorption was endothermic reaction and this was suggested to be the main reason for the behavior.

6.4 Mode of operation

Kurniawan *et al*. [33] reported some studies (Cu^{2+} removal with peanut hull for example), which showed significant improvements in adsorption capacities in column mode compared to batch studies results (65.6 mg/g and 10.2 mg/g, respectively). This behavior was explained by the different natures of column and batch studies. The concentration gradient decreases with time in batch experiments. In column operation, the adsorbent is continuously in contact with fresh feeding solution at the interface of the adsorption zone.

On the other hand, Dwivedi *et al*. [18], indicated that the adsorption capacity of GAC was far less in column mode than in batch mode. The maximum adsorption capacity achieved was in batch studies 26.5 mg/d and in column studies 2.0 mg/g (breakthrough capacity 50%). The explanation may lie with the potential irreversibility of the adsorption process. Another reason might be the different approaches to adsorption equilibrium in different systems. In bathc-mode the concentration in solution is continuously decreasing while in the column system the concentration is continuously increasing.

6.5 Effect of agitation speed and flow rate

In batch studies the greater the agitation speed the faster is the metal uptake rate. This is related to mass transfer resistance. Reducing the film boundary layer surrounding particles, thus increasing the external film transfer coefficient and the rate of metal uptake [53]. In batch studies the time is rarely limited, but this is not the case with column studies. Dwivedi [18] concluded that increase in the flow rate in the column (also called as hydraulic loading rate) causes increase in the zone speed. As a result the time required to achieve breakthrough is decreased. This causes variation in the slope of the breakthrough curve and adsorption uptake, as shown in Figure 16. Flow rates varied from 4 to 16 $m^3/(h\ m^2)$, with the maximum adsorption uptake was at flow rate value of 12 $m^3/(h\ m^2)$.

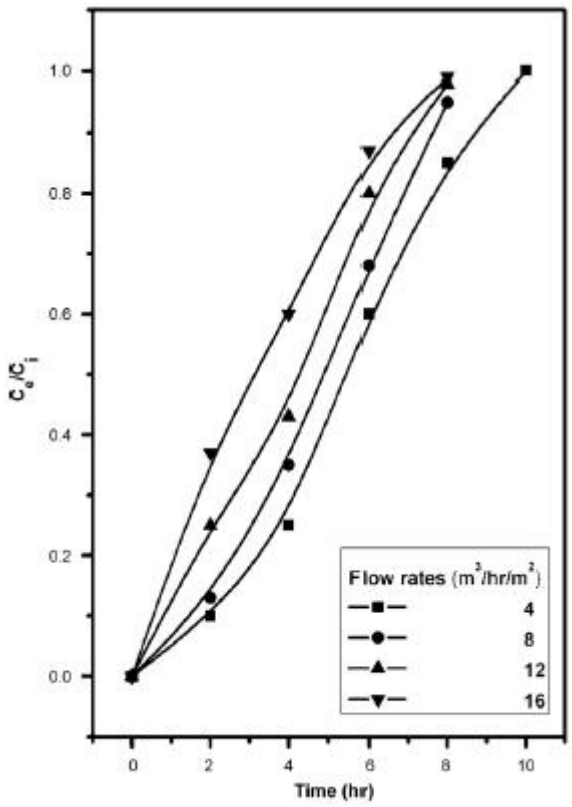

Figure 16. Breakthough curve for different hydraulic loading rates at constant feed concentration of 60 mg/L for Pb(II) removal with granular activated carbon [18].

6.6 Other factors affecting adsorption equilibria

Ahmaruzzaman [5] reported that decrease in particle size leads to increase in surface area and adsorption rate. Increase in surface area creates greater opportunities for binding heavy metals on the surface of the adsorbent. It also decreases intra-particle diffusional resistance, which is higher for larger particles. Smaller particle size increases the adsorption capacity. This becomes with the price of difficult separation of adsorbent from solution or, in the case of columns, increase in pressure drop.

Ionic strength affects the affinity between the solute and the aqueous phase. It is one important factor influencing equilibrium. In general, increasing ionic strength decreases adsorption in aqueous solution. This is especially true if the adsorption is electrostatic attraction in nature. Some inorganic anions may form complexes with some metal ions affecting adsorption. [5]

Kurniawan *et al*. [33] reported that due their small ionic radius, the Cu ions had the highest uptakes among Cu, Ni, Mn and Co removal by kaolinite. The amount of Pb(II) adsorbed was more than Cu(II) or Cd(II) in the study of Wang *et al*. [28]. This was suggested to be related to the atomic radius, which is slighty smaller for lead than for copper or cadmium. The atomic radius affects diffusivity of the metal ions and availability of sites on the surface. In another study of kaolinite, Cr(II) ions were the most readily adsorbed among the selected heavy metals (Cd^{2+}, Cr^{3+}, Cu^{2+}, Ni^{2+}, Zn^{2+}) due to its highest ionic charge compared to the others. Erdem *et al*. [10] concluded from the adsorption capacities of several metal(II)ions onto zeolites, that the adsorption capacities obeyed the order of the diameter of the metal ions. The biggest diameter of the ions had the maximum adsorption capacity. An *et al*. [23] concluded this same result with crab shell adsorbent (order of adsorption was Pb>Cu>Cd) and it was stated that the heavy metal removal was correlated by electronegativity of the ions.

One feature affecting adsorption equilibria is surface charge of the adsorbent, which is affected strongly by pH. Kurniawan [33] reported several cases, where the modification of the adsorbent resulted higher adsorption capacities. It was suggested that the main factor for this behavior was the increased negative surface charge of the adsorbent.

It should strongly emphasized that the focus of this study was on single-component adsorption. The behavior of multicomponent (or real) adsorption is vital in design of adsorption processes, but was excluded nevertheless from this study.

7 SIMULATION OF AN ADSORPTION COLUMN

7.1 General procedure of design

According to Deliyanni *et al*. [48] the major aim in designing an adsorption column is to predict the service time until the column effluent exceeds the maximum allowed pollutant concentration. The maximum effluent concentration is in many cases defined by environmental regulations. The real problem with sizing the equipment accurately is that the progress of the mass transfer zone (MTZ) introduces time into the equations. To solve these kinds of problems, it is

needed to introduce set of partial differential equations that describe the heat and mass transfer phenomena. Several shortcut methods are available but the accuracy of those methods varies. The made simplifications and the uncertainties in them often relates to conservative sizing of equipment. Various methods have been suggested for designing fixed-bed adsorption systems. The length of unused bed (LUB) theory, empty bed residence time procedure (EBRT or EBCT) are some of the most common ones employed.

7.1.1 Length of Unused Bed

The constant pattern approximation provides a simple tool for the widely used LUB theory in design. The length of the capacity of the bed that is lost as a result of the spread in concentration profile is called the length of unused bed L_{UB}. It can be calculated via the following two equations

$$L_{UB} = (1 - \frac{q_b}{q_e})L \tag{22}$$

$$L_{UB} = (1 - \frac{t_b}{t_{st}})L \tag{23}$$

where q_{b} adsorption capacity in breakthrough point

L length of column

t_{b} breakthrough time

t_{st} stoichiometric time.

The stoichiometric time describes the time needed for a stoichiometric front (the ideal case of no mass transfer resistance) to reach the end of the fixed bed. The breakthrough time and the stoichiometric breakthrough time can be calculated from overall mass balance

$$t_{st} = \frac{L}{u}\left[1 + \left(\frac{1-\varepsilon}{\varepsilon}\right)\left(\frac{q_e}{c_0}\right)\right] = \int_0^\infty \left(1 - \frac{c}{c_0}\right) dt \tag{24}$$

$$t_b = \frac{L}{u}\left[1 + \left(\frac{1-\varepsilon}{\varepsilon}\right)\left(\frac{q_b}{c_0}\right)\right] = \int_0^{t_b}\left(1 - \frac{c}{c_0}\right)dt \quad (25)$$

where u superficial flow velocity in the bed

ε porosity of the bed.

The L_{UB} is easily determined from an experimental breakthrough curve and the length of the column can be simply calculated from equilibrium considerations, if the constant pattern behaviour is assumed. [8]

7.1.2 Bed Depth Service Time Model

The Bed Depth Service Time (BDST) model relates the service time of the column to the quantity of the adsorbent in the bed, which is directly proportional to the bed height. The quantity is used instead of the bed volume, because the quantity of the bed is more accurate to measure [48]. The model is based on the study of Bohart and Adams [56]. The linear relationship between service time and bed height is

$$t_b = \frac{q_e L}{c_0 u} - \frac{1}{c_0 K_{BA}}\left[\left(\frac{c_0}{c_b}\right) - 1\right] \quad (26)$$

where K_{BA} rate constant.

The service time can be obtained with laboratory column experiments over a range of flow velocities. Hutchins [57] simplified the equation by writing it in linear form

$$t_b = a_{BA}L + b_{BA} \quad (27)$$

where

$$a_{BA} = \frac{q_e}{c_0 u} \quad (28)$$

$$b_{BA} = \frac{1}{c_0 K_{BA}} \left[\left(\frac{c_0}{c_b} \right) - 1 \right] \quad (29)$$

The parameters in Equation (26) can now be obtained by conducting experiments in different bed depths and monitoring the operating time to reach certain removal percentage of heavy metals. This is called the BDST plot and the obtained lines are called isoremoval lines. An example of the plot is shown in Figure 17. The obtained parameters can be used to design an adsorption column with different flowrates and initial concentrations. [20]

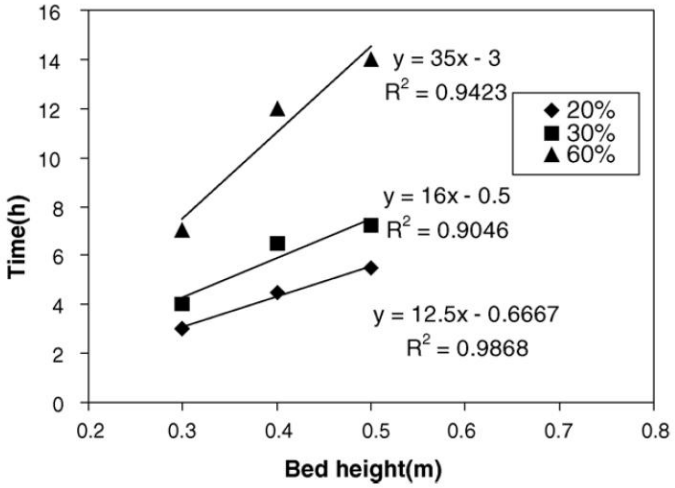

Figure 17. Bohart-Adams modelling at mini-column studies. Isoremoval lines for 20, 30 and 60% breakthrough for different bed heights. Feed concentration 6 mg/L, hydraulic loading rate 7.5 $m^3/(h\ m^2)$ [20].

Other models to predict the breakthrough curve according to Singh *et al*. [58] are the models of Thomas [59], Yoon and Nelson [60], Clark [61] and Wolbroska [62].

7.1.3 Empty Bed Residence Time model

The Empty Bed Residence Time (EBRT) is widely used design method for sizing fixed bed adsorbers. The minimum bed length is achieved by optimising the rate of the adsorbent spent (the exhaustion rate) and the EBRT operating line diagram.

The data for this optimization is obtained by the BDST or some other model used to predict the breakthrough curves (see previous chapter for details). The needed adsorbent quantity can be calculated with pre-selected breakthrough time from the selected model. In order to obtain full bed capacity, the value of 50% breakthrough is often used. This is based on the assumption that the S-shaped breakthrough curve is symmetrical in that point, which is often not the case. [48]

7.2 Mass transfer modeling

7.2.1 Basic equations for adsorption column

The equations presented in this chapter are described in the same manner as in the work of Reunanen *et al*. [63].

The mass balance for fixed bed column may be written as

$$\frac{\partial c}{\partial t} + u\frac{\partial c}{\partial z} = \frac{-(1-\varepsilon)}{\varepsilon}\frac{\partial c_s}{\partial t} \tag{30}$$

where c concentration in fluid

t time

u superficial velocity

z location in the column

ε void fraction

c_s adsorbate concentration in solids,

and the concentration in the adsorbent can be calculated from

$$c_s = \frac{\rho_s}{(1-\varepsilon)\bar{q}} \tag{31}$$

where $\bar{q}$ mean value of the concentration in the particle

ρ_s density of the solid

If effective solid diffusivity is assumed, the mass transfer rate from the surface of the particles into the particles per unit volume is equal to

$$\dot{w} = \rho_s \frac{d\bar{q}}{dt} = -aD_s\rho_b \frac{\partial q}{\partial r}|_{r=r_s} \tag{32}$$

where $\dot{w}$ mass transfer rate in the unit volume of bed

a particle surface per unit volume of bed

ρ_b density of the bed

r particle radius

where the solid concentration on the surface of the particle is determined by the adsorption equilibrium. In this case, the Freundlich adsorption equilibrium (Equation (5)) was used and where the liquid concentration on the surface is calculated from the bulk liquid concentrations as

$$\dot{w}_v = ak_f(c - c_i) \tag{33}$$

where k_f mass transfer coefficient of the fluid

c_i interface concentration

If the linear driving force assumption is used to describe the mass flow rate into the particle, then Equation (32) may be expressed the following way

$$\dot{w}_v = a\rho_s \frac{10D_s}{d_p}(q_i - \bar{q}) \tag{34}$$

where D_s diffusivity in the solid

d_p particle diameter

q_i concentration in the solids at the interface

where the solid-side mass-transfer coefficient k_s is described by the term $10D_s/d_s$. [63]

The mass transfer coefficient between the fluid and the particles in packed bed is obtained from empirical correlations found in the literature. Fujiki *et al*. [64] mentioned some widely used correlations in their study. These included empirical correlations from Wilson-Geankoplis, Carberry, Syohdia-Ramswami-Hougen and Wakao-Funazkri. The Wakao and Funanzkri [65] experimental correlation was used in this study. It is expressed with dimensionless numbers as

$$Sh = \frac{k_f d_p}{D_m} = 2 + 1.1 Sc^{1/3} Re_p^{0,6} \quad (35)$$

where Sh Sherwood number

Sc Schmidt number

Re_p particle Reynolds number

D_m diffusivity in the fluid

The particle Reynolds number is defined

$$Re_p = \frac{\rho_f u d_p}{\mu_f (1-\varepsilon)} \quad (36)$$

where ρ_f density of the fluid

μ_f viscosity of the fluid.

Diffusivity in fluid can be calculated with general correlations from the literature [66]. The value for effective diffusivity cannot be solved theoretically and it must be calculated from experimental data. D_{eff} can be determined by carrying out adsorption experiments in stirred vessels (batch study). These studies are conducted in controlled conditions and the value of D_{eff} is obtained from the kinetic data (usually a plot time versus concentration/reduced concentration). The external film mass transfer is often negligible (with high stirring speeds), which

simplifies the calculations. The assumption should always be verified with column studies. [67]

Reunanen [63] presented the methods of Crank [68], Rice [69] and Huang and Li [70] for determination of effective diffusivity from batch experiments. If the adsorption is controlled by intra-particle pore diffusion, the values for D_{eff} can be obtained from intraparticle diffusion kinetic model (Equation (13)) with a simple equation [46].

Another approach to determine effective diffusivity is the fixed bed adsorption breakthrough curve method. According to Sonetaka *et al.* [71] the method uses empirical correlations to estimate the fluid-film resistance, which may result some error to calculations. To improve the results a shallow bed reactor (high flow velocity) may be used, which neglects the liquid film resistance. This assumption might not be valid for particles with small diameter. Sonetaka *et al*. suggested a new analytical method for obtaining values for both effective diffusivity and liquid film mass transfer coefficient from adsorption uptake curve. This method was later expanded for the use of completely mixed batch reactors by Fujiki *et al*. [72].

7.2.2 Analytical solutions for breakthrough curve

Calculation of adsorption breakthrough curve can be carried out analytically. These solutions are based on multiple simplifying assumptions. Perhaps the most well-known solution for solving adsorption problem analytically was represented by Rosen [73]. The method assumes that adsorption isotherm is linear (Henry's isotherm), which is often not the case with heavy metal adsorption for aqueous solutions. Thomas [74] presented an analytical solution for nonlinear adsorption isotherm following Langmuir isotherm. The assumptions used in the solution are listed below (according to Reunanen [63]):

- pressure and temperature are constant in the column
- adsorption isotherm is nonlinear (Langmuir's isotherm)
- diffusion resistance in the particle is noted
- thickness of the diffusion layer in the particle is constant

- axial dispersion in the column is neglected
- concentration in cross-section area is constant
- mass transfer in the fluid side is taken into account
- mass transfer coefficient in the surface film is constant
- fluid velocity is constant all over the column
- adsorbing particles are spherical and equal size

Some other analytical solutions are for example the ones developed by Liaw [75], Rasmuson [76] and Rice [77].

7.2.3 Numerical solution for breakthrough curve

There are several ways to calculate the adsorption breakthrough curve by numerical methods. The simulation program used in the study is a program by Reunanen *et al*. [6]. The model equations are described in the previous chapter 7.2.1. More detailed description of the simulation program can be found from the original article. The method is a numerical solution of the breakthrough curve in an adsorption column. It should provide good accuracy and a considerable reduction in the computing time. The parameters required for the simulation program are presented in Table VI in the next chapter.

7.2.3 Parameters for simulation

Motsi *et al*. [78] presented some concentrations of heavy metals found form acid mine drainage. The concentration in heavy metals in the samples were 200 (Fe^{3+}), 85 (Zn^{2+}), 12 (Cu^{2+}), 15 (Mn^{2+}), 15 (Al^{3+}), 15 (As^{3+}) and 9 (Cd^{2+}) mg/L. The initial concentration of 20 mg/L for a single component adsorption was selected for this study to be representative of the situation in reality. The superficial flow velocity in the column was chosen as 0.139 mm/s (0.5 $m^3/(h\ m^2)$). Naiya *et al*. [30] researched the use of activated alumina for removal of Cd(II) and Pb(II) ions with adsorption from aqueous solutions, and this study was selected as the base for the simulation case. The properties of the activated alumina are listed in Table V. The void fraction was estimated to be 0.45.

Table V. Properties of the activated alumina and some information about the batch studies conducted by Naiya *et al.* [30].

Properties of activated alumina
Used particle size 250 - 350 μm
Effective diameter 291.45 μm
BET surface area 126 m^2/g
Bulk density 0.81 g/cm^3
Langmuir constants:
Cd(II): q_m = 35.06 mg/L, b = 0.1389 L/mg
Pb(II): q_m = 83.33 mg/L, b = 0.0515 L/mg
Freundlich constants:
Cd(II): K_f = 4.34 (mg/g)/(mg/L)$^{1/n}$, n = 1,81
Pb(II): K_f = 3.82 (mg/g)/(mg/L)$^{1/n}$, n = 1,44

The constants of Freundlich adsorption isotherms were used. The values for viscosity and fluid density are assumed the same as for pure water in 25 °C. The used values for simulation are shown in the in Table VI.

Table VI. Parameters required for the simulation program and the values used in this study.

Parameter	Unit	Values used in study
Solute concentration of the feed	kg,m^3	20
Bulk density of the bed	kg/m^3	810
Void fraction of the bed	-	0.45
Effective diffusivity in the particles	m^2/s	$1.096 \cdot 10^{-10}$ (Cd^{2+}) $1.39 \cdot 10^{-10}$ (Pb^{2+})
Superficial flow velocity of the fluid	m/s	$1.39 \cdot 10^{-4}$
Diameter of the particles	m	$291 \cdot 10^{-6}$
Coeffiecient (K) of the Freundlich isotherm	$kg_{Me}/kg_{Adsorbent}$	0.00434 (Cd^{2+}) 0.00382 (Pb^{2+})
Exponent of the Freundlich isotherm	-	1/1.81 (Cd^{2+}) 1/1.44 (Pb^{2+})
Fluid density	kg/m^3	1000
Height of bed	m	variable
Fluid viscosity	kg(m s)	0.001
Diffusivity in fluid	m^2/s	$7.19 \cdot 10^{-10}$ (Cd^{2+}) $9.45 \cdot 10^{-10}$ (Pb^{2+})

7.3 Simulation results

The target was to run the column for 24 hours and treat 100 m^3 of wastewater per day. Two separate simulations were executed: one with water containing Cd(II) ions and one with Pb(II) polluted water. When the column effluent pollutant concentration reaches a certain level, the column is regenerated. This breakthrough point was set to be 10% of the initial concentration (2 mg/L). The appropriate height for the column was searched by trial and error method. The column was sized accordingly and the results are shown in Table VII. The breakthrough curves are shown in Figure 18.

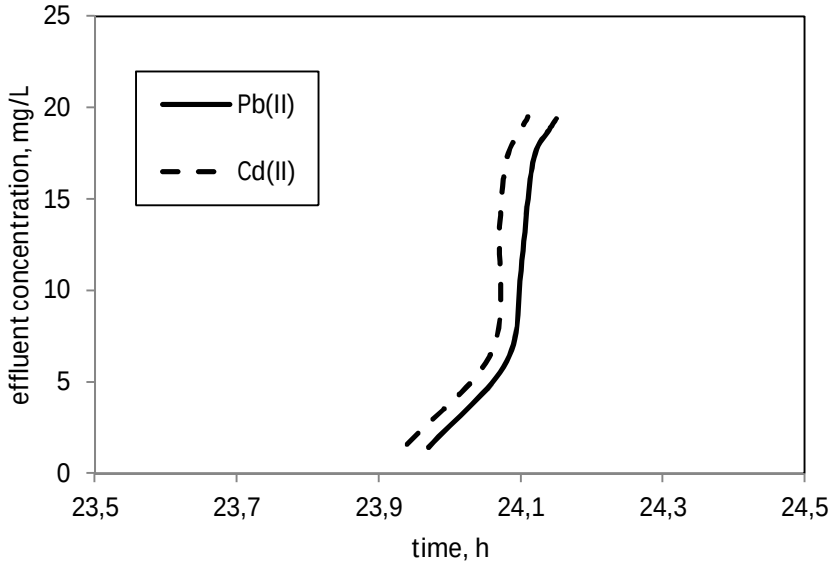

Figure 18. Breakthrough curves for Pb(II) and Cd(II) adsorption with activated alumina. Hydraulic loading rate 4.17 $m^3/(h\ m^2)$, initial metal ion concentration 20 mg/L. Height of the bed 13.38 m for Cd(II) and 9.40 m for Pb(II).

As observed from Figure 18 the shape of the breakthrough curve is really steep. The adsorption is favorable and the mass transfer zone is relatively short. It was found that with certain parameter values some stability problems occurred during simulations.

Table VII. Results for simulated adsorption column with activated alumina. Hydraulic loading rate 4.17 $m^3/(h\ m^2)$, initial metal ion concentration 20 mg/L.

	Cd^{2+}	Pb^{2+}
Height of column, m	13.38	9.40
Diameter of column, m	3.26	3.26
Required amount of adsorbent, kg	15,886	11,160

The selected adsorbent is moderate or below moderate adsorbent of removing heavy metal ions from waters. For the sake of comparison, the maximum

adsorption capacity in the study was 35.06 mg/g for Cd(II) and 83.33 mg/g for Pb(II) ions. Only one value of D_{eff} was given for the intra-particle diffusion, although in many studies it is clearly observed that this value varies with different intial concentrations. The initial concentrations reported in the study were 10, 25 and 50 ppm, which are in perfect agreement with the chosen concentration for the simulation. In the reference [30] it was stated that the sorption was controlled by film diffusion (according to Richenberg model) and on the other hand it was stated that the diffusion of adsorbate into the pores of the adsorbent is not solely the rate-limiting step (according to Bangham's equation). To confirm, if the simulated situation is strongly affected by variation in the D_{eff}, a sensitivity analysis was performed. The results are shown in Figures 19 - 20.

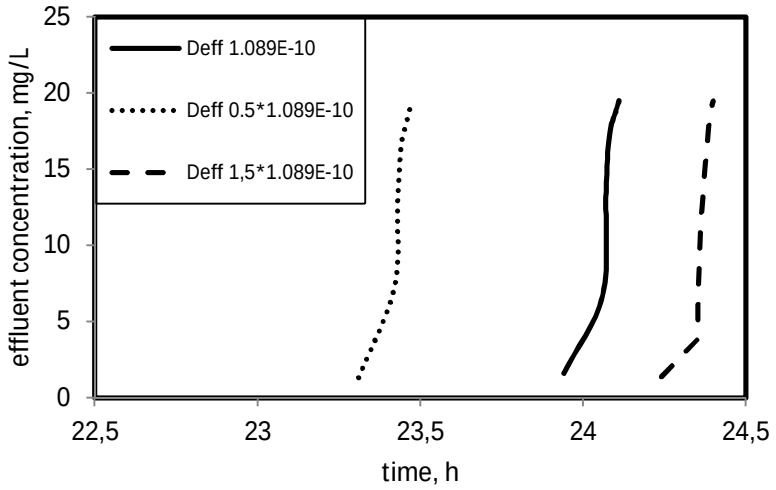

Figure 19. Sensitivity analysis on Cd(II) adsorption by varying D_{eff} ±50%. Hydraulic loading rate 4.17 $m^3/(h\ m^2)$, initial metal ion concentration 20 mg/L. Height of the bed 13.38 m.

When the effective diffusivity was decreased by 50%, the breakthrough time decreased about 0.6 hours with cadmium ion removal. On the contrary, by increasing the D_{eff} by 50%, the breakthrough time increased only about 0.3 hours. The effect with lead ion removal was less severe. Decrease of 0.15 and increase of 0.3 hours by varying D_{eff} -50% and +50%, respectively, was observed. This clearly indicates that effective diffusivity may be an important factor in the design of adsorption column. Some values reported in the literature [30] for chemisorption system (as this was concluded to be in the reference) range from

10^{-9} to 10^{-17} m^2/s. Besides these uncertainties, no data of fit of the D_{eff} was available in the reference [30].

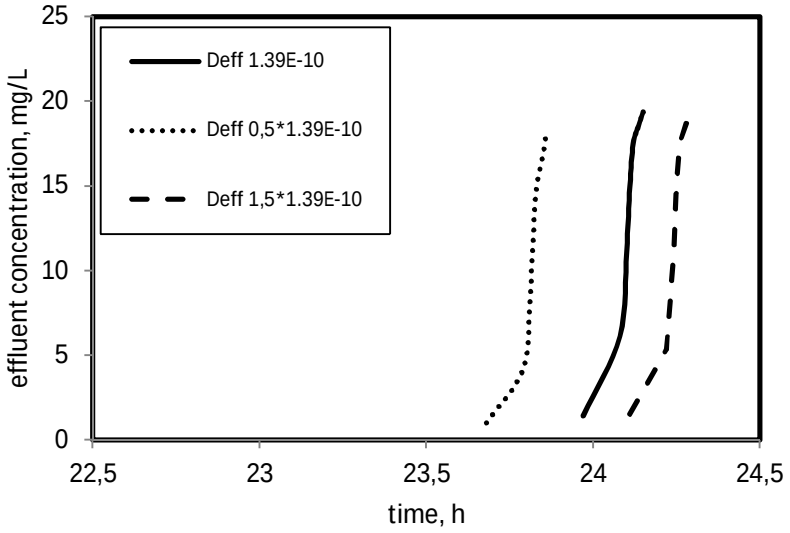

Figure 20. Sensitivity analysis on Pb(II) adsorption by varying D_{eff} ±50%. Hydraulic loading rate 4.17 $m^3/(h\ m^2)$, initial metal ion concentration 20 mg/L. Height of the bed 9.40 m.

The dimensions of the two columns designed are shown in Table VII and results are rather unpromising. The columns are physically large and lots of adsorbent material is needed in the column. This combined with the need of regeneration of every 24 hours and the loss of adsorption capacity reported in the reference [30], makes the adsorption process seem unfeasible. It should also be noted that the operation with real multicomponent solutions is not exactly known and the dimensions of the columns are always larger in multicomponent systems. Although, Naiya *et al*. [30] were successful of treating an industrial effluent containing 3.8 mg/L Cd(II). Adsorption capacities in batch and fixed-bed operation have varied from study to study and this aspect of the adsorption behavior of activated alumina could be worth investigating.

Other uncertainties in the simulation were the estimated value for porosity, suitability of the empirical correlation of the external mass transfer and applicability of the use of the Freundlich isotherm (the Langmuir isotherm suited the results better).

To obtain more reliable results, laboratory scale experiments should be conducted. Batch studies combined with for example mini-column studies to confirm the results and obtain parameters in the EBCT method are recommended. The fine tuning of the used program for specifically to the conditions of heavy metal removal from aqueous solutions, would improve the reliability and usability of the software greatly.

8 CONCLUSIONS

The purpose of the work was to study the feasibility of the adsorption for removal of various heavy metals from aqueous solutions. The focus was on single component adsorption of Cu(II), Cd(II) and Pb(II) ions. In the theoretical part different types of heavy metal adsorption mechanisms, materials and their adsorption capacities were introduced. The regeneration and factors affecting the adsorption equilibria were discussed and the most common adsorption isotherms and kinetic models were represented. In the latter part of the study, some mass transfer models were introduced and the general procedure of design was illustrated with few well-known methods. Two single component adsorption columns were simulated and sized with numerical software. The parameters for simulation were selected from the literature.

The adsorption of heavy metal is rather effective method to remove heavy metals from water in the range of less than 1000 mg/L of heavy metals in aqueous solutions. The mechanisms of adsorption are dependent on the used adsorbent and the sorption process can be attributed to physical adsorption, chemisorption and ion-exchange. The range of various adsorbents being used and studied in the literature is wide. Activated carbon seems to be the most used one in industry for its applicability in several situations. The main focus of the new literature studies was noted to be focused on search of a low-cost adsorbent due to the price increase of traditionally used activated carbon. The uptake capacities varied from less than 1 to over 1000 $mg_{metal}/g_{adsorbent}$. The selection of suitable adsorbent is always case dependent. Adsorbents can be regenerated effectively with mineral acids although durability of regeneration of adsorbents is an issue in many cases. The Freundlich and Langmuir adsorption isotherms were the most widely used isotherms and Langmuir fit the data better in majority of the articles. Pseudo-

second-order reaction rate equation fitted the data decently almost in every reported study. The pH was found out to be the most dominant factor affecting heavy metal adsorption capacities of all other operation conditions. In general the most optimal pH was found to be about 5-6.

The design of the adsorption column with the presented simulation program was found to be challenging due to the difficulties in obtaining the necessary model parameters from the literature only and therefore series of laboratory experiments are recommended. The simulation was done for Cd(II) and Pb(II) for a specific removal case. The results indicated requirement of rather large equipment and the feasibility of the designed adsorption processes is therefore questionable. Stability issues were found during simulations and therefore the used program is not be suitable for simulations of heavy metal removal from aqueous solutions in all cases. Several uncertainties were discussed and laboratory measurements both in batch and in fixed-bed operation are recommended for a detailed study.

REFERENCES

1. Paulino, A.T., Minasse, F.A.S., Guilherme, M.R., Reis, A.V., Muniz, E.C., Nozaki, J., Novel adsorbent based on silkworm chrysalides for removal of heavy metals from wastewaters, *J. Colloid Interface Sci.* **301** (2006), 479-487.
2. Fu, F., Wang, Q., Removal of heavy metal ions from wastewaters: A review, *Journal of Environmental Management* **92** (2011), 3, 407-418.
3. Lenntech: WHO/EU drinking water standards comparative table, http://www.lenntech.com/who-eu-water-standards.htm [16.10.2012]. W
4. Handbook of Environmental Engineering, Vol 11, Wang, L.K., ed, Spinger e-books, p. 375 – 402.
5. Ahmaruzzaman, M., Industrial wastes as low-cost potential adsorbent for wastewater laden with heavy metals, *Advances in Colloid and Interface Science* **166** (2011), 36-59.
6. Reunanen, J., Palosaari, S., Miyhara, M., Okazaki, M., Reliable numerical calculation of the breakthrough curve of an adsorption column, *Chemical Engineering and Processing: Process Intensification* **33** (1994), 3, 117-123.
7. Richardson, J.F., Harker, J.H., Backhurst, J.R., *Coulson & Richardson's Chemical Engineering*, Vol 2, 5th ed., Elsevier, 2002, p. 970-1052.
8. *Kirk-Othmer Concise Encyclopedia of Chemical Technology*, Vol 1, , 5th ed., John Wiley & Sons, New Jersey, 2007, p. 56-69.
9. *Kirk-Othmer Encyclopedia of Separation Technology*, Vol 1, Ruthven, D., ed., John Wileys & Sons, New York, 1997, p. 94-129, 172-199.
10. Erdem, E., Karapinar, N., Donat, R., The removal of heavy metal cations by natural zeolites, *Journal of Colloid and Interface Science* (2004) **280**, 309-314.
11. Lyubchik, S., Khorokovskij, M., Makavrova, T., Tikhonova, L., Mota J.P.B., Fonseca, I., Waste conversion into activated carbon for heavy metal removal from waste water, *Recent Advances in Adsorption Processes for Environmental Protection and Security* NATO Science for Peace and Security Series C: Environment Security, Springer e-books, 2008, p. 133-146.
12. Kumar, G.P., Kumar, P.A., Chakraborty, S., Ray, M., Uptake and desorption of copper ion using functionalized polymer coated silica gel in aqueous environment, *Separation and Purification Technology* **57** (2007), 47-56.
13. Barakat, M.A., Adsorption behavior of copper and cyanide ions at TiO2–solution interface, *J. Colloid Interface Sci.* **291** (2005), 345– 352.
14. Barakat, M.A., New trends in removing heavy metals from industrial wastewater, *Arabian Journal of Chemistry* **4** (2011), 361-377.
15. Yin, C.Y., Aroua, M.K., Daud. W.M.A.W., Review of modifications of activated carbon for enhancing contaminant uptakes for aqueous solutions, *Separation and Purification Technology* **52** (2007), 403-415.
16. Turan, M., Mart, U., Yüksel, B., Celik, M.S., Lead removal in fixed-bed columns by zeolite and sepiolite. *Chemosphere* **60** (2005), 1487-1492.
17. *Handbook of Separation Process Technology*, Rousseau, R.W., ed., Wiley, New York, 1987, p. 183-190.

18. Dwivedi, C.P, Sahu, J.N., Mohanty, C.R., Mohan, B.R., Meikap, B.C., Column performance of granular activated carbon packed bed for Pb(II) removal, *Journal of Hazardous Materials* **156** (2008), 596-306.
19. Suzuki, M., *Adsorption Engineering*, Elsevier, Kodansha, 1990, p.13-14.
20. Goel, J., Kadirvelu, K., Rajagopal, C., Garg, K.V., Removal of lead(II) by adsorption using treated granular activated carbon: Batch and column studies, *Journal of Hazardous Materials* **B125** (2005), 211-220.
21. Uzun, Í., Güzel, F., Adsorption of Some Heavy Metal Ions from Aqueous Solution by Activated Carbon and Comparison of Percent Adsorption Results of Activated Carbon with those of Some Other Adsorbents, *Turkish Journal of Chemistry* **24** (2000), 291-297.
22. Marinkovski, M., Markovska, L., Meshko, V., Equilibrium studies of Pb(II), Zn(II) and Cu(II) ions onto granular activated carbon and natural zeolite, *Chemicals as Intentional and Accidental Global Environmental Threats NATO Security through Science Series*, 2006, Springer, p. 477 – 486.
23. An, H.K., Park, B.Y., Kim, D.S., Crab shell for the removal of heavy metals from aqueous solution, *Wat. Res.* **35** (2001), 3551-3556.
24. Leyva-Ramos, R., Berber-Mendoza, M. S., Salazar-Rabago, J., Guerrero-Coronado, R. M., Mendoza-Barron, J., Adsorption of lead(II) from aqueous solution onto several types of activated carbon filters, *Adsorption* **17** (2011), 3, 515-526.
25. Tran, H.H., Roddick, F.A., Comparison of chromatography and desiccant silica gels for the adsorption of metal ions – II. Fixed-bed study, *Wat. Res.* **33** (1999), 3001-3011.
26. Barakat, M.A., Sahiner, N., Cationic hydrogels for toxic arsenate removal from aqueous environment, *J. Environ. Manage.* **88** (2008), 955–961.
27. Krusic, M.K., Milosavljevic, N., Debelkovic, A., Üzüm, Ö.B., Karadag, E., Removal of Pb2+ ions from water by poly(acrylamide-co-sodium methacrylate) hydrogels, *Water air soil pollution* **223** (2012), 4355-4368.
28. Wang, J., Liu, F., Wei, J., Enhanced adsorption properties of interpenetrating polymer network hydrogels for heavy metal ion removal, *Polym. Bull*. **67** (2011), 1709-1720.
29. Wang , J., Xu, L., Meng, Y., Cheng, C., Li, .A, Adsorption of Cu^{2+} on new cross-linked polystyrene adsorbent: Batch and column studies, *Chemical Engineer Journal* **178** (2011), 108-114.
30. Nayia, T.K., Bhattacharya, A.K., Das, S.P., Adsorption of Cd(II) and Pb(II) from aqueous solutions on activated alumina, *Journal of Colloid and Interface Science* **333** (2009), 14-26.
31. Liu, X.-W., Wang, J.-R., Hu, Y.-H., Adsorption of copper(II) and chromium(IV) on diaspore, *J. Cent. South Univ. Technol*. **15** (2008), 515-519.
32. Hua, M., Zhang, S., Pan, P., Zhang, W., Lv, L., Zhang, Q., Heavy metal removal from water/wastewater by nanosized metal oxides: A review, *Journal of Hazardous Materials* **211-212** (2012), p. 317-331.
33. Kurniawan, T.A., Chan, G.Y.S., Lo, W-H., Babel, S., Comparisons of low-cost adsorbents for treating wastewaters laden with heavy metals, *Science of the Total Environment* **366** (2006), 409-426.
34. Gupta, S.S., Bhattacharyya, K.G, Interaction of metal ions with clays: I. A case study with Pb(II), *Applied Clay Science* **30** (2005), 199-208.

35. Bhattacharyya, K.G., Gupta, S.S., Kaolinite, montmorillonite, and their modified derivatives as adsorbents for removal of Cu(II) from aqueous solution, *Separation and Purification Technology* **50** (2006), 388-397.
36. Wang, J., Chen, C, Biosorbents for heavy metal removal and their future, *Biotechnology Advances* **27** (2009), 195-226.
37. Singh, A., Mehta, S.K., Gaur, J.P., Removal of heavy metals from aqueous solution by common fresh water filamentous algae, *World J. Microbiol. Biotechnol.* **23** (2007), 1115-1120.
38. *Ullmann's Encyclopedia of Industrial Chemistry*, Vol B3, Gerhartz W., ed., 5th ed., VCH, Würzburg, 1988, p. 9-1 - 9-52.
39. Gupta, V.K., Srivastava, D., Mohan, D., Sharma, S., Design parameters for fixed bed reactors of activated carbon developed from fertilizer waste for the removal of some heavy metal ions, *Waste management* **17** (1997), 8, 517-522.
40. Singh, A., Kumar, D., Gaur, J.P., Removal of Cu(II) and Pb(II) by *Pithophora oedogonia*: Sorption, desorption and repeated use of the biomass, *Journal of Hazardous Materials* **152** (2008), 1011-1019.
41. Kumar, U., Bandyuopadhyay, M., Fixed-bed column study for Cd(II) removal from wastewater using treated rice husk, *Journal of Hazardous Materials* **B129** (2006), 253-259.
42. Katsou, E., Malamis, S., Tzanoudaki, M., Haralambous, K.J., Loizidou, M., Regeneration of natural zeolite polluted by lead and zinc in wastewater systems, *Journal of Hazardous Materials* **189** (2011), 773-786.
43. Saha, B., Chakraborty, S., Das, G., A comperative metal ion adsorption study by trimesic acid coated alumina: A potent adsorbent, *Journal of Colloid and Interface Science* **323** (2008), 26-32.
44. Shahbazi, A., Younesi, H., Badiei, A., Funcionalized SBA-15 mesoporous sica by melamine-based dendimer amines for adsorptive characteristcs of Pb(II), Cu(II) and Cd(II) heavy metal ions in batch and fixed bed column, *Chemical Engineering Journal* **168** (2011), 505-518.
45. Redlich, O., Peterson, D.L., A useful adsorption isotherm, *J. Phys. Chem.* **63** (1959), 1024.
46. Debnath, S., Ghosh, U.C., Equilibrium modeling of single and binary adsorption of Cd(II) and Cu(II) onto agglomerated nano structured titanium(IV) oxide, *Desalination* **273** (2011), 330-342.
47. Bruanuer, S., Emmett, P.H., Teller, E., *J. Am. Chem. Soc.* **38** (1938), 309.
48. Deliyanni, E.A., Peleka, E.N, Matis, K.A., Modeling the sorption of metal ions from aqueous solution by iron-based adsorbents, *Journal of Hazardeous* Materials **172** (2009), 550-558.
49. Lagergren, S., Zur theorie der sogenannten adsorption geloster stoffe, *Stoffe Kungliga Svenska Vetenskapskademiens*, Handlingar **24** (1898), 1–39.
50. Ho, Y.S. , McKay, G., Kinetic models for the sorption of dye from aqueous solution by wood, *Proc. Safety Environ. Protect.* **76** (1998), 183–191.
51. W.J. Weber Jr., J.C. Morris, Kinetics of adsorption on carbon from solution, *J. Sanit. Eng. Div.*, ACSE **89** (1963) 31–59.
52. Roginsky, S.Z., Zeldovich, J., *Acta Physicochim* USSR **1** (1934), 554.

53. Kocaoba, S., Orhan, Y., Akyüz, T., Kinetics and equilibrium studies of hevay metal ions removal by use of natural zeolite, *Desalination* **214** (2007), 1-10.
54. Thomas, W.J., Crittenden, B., *Adsorption Technology and Design*, Butterworth/Heinemann, Oxford, 1998, pp. 38–50.
55. Kocaoba, S., Comparison of Amberlite IR 120 and dolomite's performance for removal of heavy metals, *Journal of Hazardous Materials* **147** (2007), 488-496.
56. Bohart, G.S., Adams, E.Q., Some aspects of the behaviour of charcoal with respect to chlorine, *J. Am. Chem. Soc.* **42** (1920), 523-544.
57. Hutchins, R.A., New Method simplifies design of activated carbon systems, *Chemical Engineering* **80** (1973), 133-138.
58. Singh, S., Srivastava, V.C., Mall, I.D., Fixed-bed study for adsorptive removal of furfural by activated carbon, *Colloids Surf. A* **332** (2009), 50-56.
59. Thomas, H.C., *J. Am. Chem. Soc.* **66** (1944), 1664.
60. Yoon, Y.H., Nelson, J.H., *Am. Ind. Hyg. Assoc. J.* **45** (1984), 509.
61. Clark, R.M., *Environ. Sci. Tecnol.* **21** (1987), 573.
62. Wolbroska, A., *Water Res.* **23** (1989), 85.
63. Reunanen, J., Adsorptiokäyrän läpäisykäyrän laskenta (Calculation of the adsorption breakthrough curve), Lic. Sc. (Tech.), Lappeenrannan teknillinen korkeakoulu, Lappeenranta, 1992, p. 23-52.
64. Fujiki, J., Shinomiya, T., Kawakita, T., Ishibashi, S., Furua, E., Experimental determination of fluid-film mass transfer coefficients from adsorption uptake curve, *Chemical Engineering Journal* **173** (2011), 49-54.
65. Wakao, N., Funazkri, T., Effect of fluid dispersion coeffcients on particle-to-fluid mass transfer coefficients in packed beds, *Chem. Eng. Sci.* **33** (1978), 1375-1384.
66. Haynes, W.M., ed., *CRC Handbook of Chemistry and Physics*, 93rd Edition (Internet Version 2013), CRC Press/Taylor and Francis, Boca Raton, FL.
67. Martins, A., Mata, T.M., Gallios, G.P., Václavíková, M., Stefusova, K., Modeling and simulation of heavy metals removal from drinking water by magnetic zeolite, in *Water Treatment Technologies for the Removal of High-Toxicity Pollutants*, Václavíková, M. *et al*., eds., Springer, 2010, p. 61 – 84.
68. Crank, J., *The Mathematics of Diffusion*, 2nd ed., Clarendon Press, Bristol, 1986, 93-96.
69. Rice, R.G., Approximate Solutions for Batch, Packed Tube and Radial Flow Adsorbers – Comparison with Experiment, *Chem. Engng. Sci.* **37** (1982), 83-91.
70. Huang, T.-C., Li, K.-Y., Ion-Exchange Kinetics for Calcium Radiotracer in a Batch System, *Ind. Eng. Chem. Fundam.* **12** (1973), 50-55.
71. Sonetaka, N., Fan., H.J., Kobayashi, S., Chang, H.N., Furua, E., Simultaneos determination of intraparticle diffusivity and liquid film mass transfer coefficient from single-component adsorption uptake curve, *Journal of Hazardous Materials* **164** (2009), 1447-1541.
72. Fujiki, J, Sonetaka, N., Ko, K.-P., Furua, E., Experimetnal determination of intraparticle diffusivity and fluid mass transfer coefficients using batch contactors, *Chemical Engineering Journal* **160** (2010), 683-690.

73. Rosen, J.B, Kinetics of a Fixed Bed System for Solid Diffusion into Spherical Particles, *J. Chem. Phys*. **20** (1952), 387-394.
74. Thomas, H.C., Ref. Sherwood, T.K., Pigford, R.L, Wilke, C.R., *Mass Transfer*, McGraw- Hill Book Company, New York, 1975, 565-585.
75. Liaw, C.H., Liquid Phase Adsorption in Fixed Beds, Ph.D. Thesis, Purdue University, 1977, 46-56.
76. Rasmuson, A., Time Doman Solution of a Model for Transport Processes in a Disperse Structured Catalyst, *Chem. Eng. Sci*. **37** (1982), 787-788.
77. Rice, R.G., Approximate Solutions for Batch, Packed Tube and Radial Flow Adsorbers – Comparison with Experiment, *Chem. Eng. Sci*. **37** (1982), 83-91.
78. Motsi, T., Rowson, N.A., Simmons, M.J.H., Adsorption of heavy metals from acid mine drainage by natural zeolite, *Int. J. Miner. Process.* **92** (2009), 42-48.